Chapter 3

Estimation of Air Fraction Profiles in the Stabilized Froth and Froth Regions of a Flotation Column Using Conductivity Probes

3.1 Introduction

In the collection zone of a flotation column, the air holdup is known to be relatively constant along the column height. The effect of the decrease in hydrostatic pressure with height may need to be taken into consideration, particularly for tall industrial columns. However, this phenomenon is readily ascertained. On the other hand, the changes at the pulp-froth interface, as well as the air fraction profile in the stabilized froth and froth zones, are still the subjects of investigation. An abrupt transition in air fraction at the interface is normally observed, while the bubble size starts increasing at the base of the froth, reaching a value of about two millimeters (Yianatos et al., 1986; Biswal et al, 1994). Above the wash-water-addition point, the average bubble size grows rapidly and the air fraction generally increases to values greater than 0.8 (Yianatos et al., 1986).

The estimation of holdup through the measurement of electrical conductivity is a method that has been widely utilized in the study of two-phase systems. The ratio between the conductivity of an air-liquid mixture and the conductivity of the liquid is a function of the air holdup. Secondly, this ratio is determined by the relative increase in the length of the path between the electrodes due to the presence of air. Some authors refer to this increase in the effective path as tortuosity (Yianatos, Laplante, Finch, 1985). Utilization of conductivity probes in flotation columns has been reported previously as part of the search for alternative measurement techniques for interface level (Moys and Finch, 1988; Gomez et al., 1989; Bergh and Yianatos, 1991; Uribe-Salas et al., 1991; Perez, del Villar, Flament, 1993) and for a method to estimate bias flow (Uribe-Salas, Gomez and Finch, 1991b). Several probe designs have also been applied to the analysis of air or solids holdup in two-phase systems. For instance, Xu, Finch and Huls (1992) have utilized conductivity probes for studying the shape of the radial air holdup profiles in flotation columns as it relates to different bubble generation devices. Others have examined the axial profile along the collection region or the stabilized froth in gas-liquid columns (Yianatos et al., 1985; Yianatos et al., 1986; Gomez et al., 1991; Uribe-Salas, Gomez and Finch, 1991; Xu et al., 1991; Marchese et al., 1992; Gomez et al., 1995). However, studies on the differences between the measured air fraction profiles in two-phase and three-phase systems, and on experimental air holdup profiles of the froth section above the wash water sprinkler have not been reported.

Consequently, an objective of this study was to observe the transition in air fraction across the interface and the increase in air fraction along the stabilized froth, with

and without solids in the system. Another objective was to attempt to determine how a draining froth profile differs from the one observed in the stabilized froth region, under various conditions. The effect of solids loading on the profiles was of particular interest.

3.2 Experimental Setup

Two conductivity probes were built to obtain an empirical estimate of the air fraction profile across the interface, along the stabilized froth and in the draining froth. It was expected that the conductivity of the air-liquid mixture would decrease from the conductivity of the liquid alone in proportion to the air volume fraction.

The stabilized froth probe consists of eleven stainless steel ring electrodes. The electrodes are separated by cylindrical sections of insulating Teflon about 1.9 centimeters long. Each ring is separated from its counterpart by a Teflon disk. The rings have an internal diameter of about 1 centimeter and are 0.38 centimeter wide. The distance between a pair of rings forming an electrode is also 1 centimeter. The probe is held together by an outer Plexiglas cylindrical sheath that extends about 44 centimeters, with an internal diameter just slightly larger than the rings in order to keep them securely in place. Before each experiment, the probe was positioned inside a laboratory column, just below the wash-water addition point. A diagram of the probe is provided in Figure 3.1. The utilization of ring electrodes was previously reported by Gomez et al. (1990), who developed a level detection probe based on a commercially-available electrode with four sensor rings. Another kind of conductivity-based probe for level measurement consisted of sequential ring-type electrodes (Perez, del Villar, Gomez, Finch, 1994). In addition, Summers, Xu and Finch (1993) utilized a ring-electrode probe for the on-line measurement of air fraction in a Jameson cell.

In the draining froth, the maximum height that can be obtained without the froth collapsing for the range of operation in the bubbly flow regime is rather limited. For this reason, a much smaller probe was used with the intention of determining the air fraction profile in that region. The geometry of the conductivity cells was changed to approximate an ideal cell consisting of two infinite parallel plates, as depicted in Figure 3.2. The probe is made up of five electrodes, and each electrode consists of two parallel copper plates about 0.76 centimeter wide on each side. The support is made out of a plastic material for insulation, and the spacing between the cells is around one centimeter. Xu, Finch and Huls (1992) had tested the accuracy of this type of electrode by comparing air fraction measurements obtained with pressure transducers to the ones obtained with the conductivity cell. The agreement was found to be very good.

Conductance measurements along the froth regions were performed using an analog multiplexer. Each electrode was selected in turn and the measurement recorded until all electrodes along the probe were scanned. The scanning was conducted as quickly as possible within the limits of the response time of the conductance meter.

Air fraction can be estimated from conductivity measurements using any of several models, including Maxwell's equation and Weissberg's tortuosity model. In these expressions, a ratio of conductivities is involved. However, conductivity differs from the measured conductance by a factor dependent on the electrode geometry. Thus, in order to utilize conductance measurements for estimating air fraction, the electrode design must be kept the same for the measurements with and without air. In this way, the ratio of conductances approximates the conductivity ratio.

3.3 Two-Phase System

In the two-phase system, the conductivity ratio is calculated by dividing the conductivity measured by any given electrode in the presence of bubbles by the one measured by the same electrode when immersed in water. In general,

$$\frac{k_{mixture}}{k_{liquid}} = \frac{1-\varepsilon}{\xi} \qquad [1]$$

where ε is the air fraction, ξ is the tortuosity term, and k is conductivity.

The oldest model still in use that relates holdup to the conductivity ratio is Maxwell's equation (Maxwell, 1892), which states that

$$\frac{k_{mixture}}{k_{liquid}} = \frac{1-\varepsilon}{1+0.5\varepsilon} \qquad [2]$$

Assuming that cell geometry is the same for all measurements and that conductivity can be substituted with the conductance measurements (K), the air holdup is given by:

$$\varepsilon = \left(\frac{1-\frac{K_{air-water}}{K_{water}}}{1+0.5\frac{K_{air-water}}{K_{water}}} \right) \qquad [3]$$

Attempts to find models applicable to various ranges of solids or gas holdup have resulted in several other expressions such as the one developed by Weissberg (1963) for overlapping spheres (applicable for high air fractions):

$$\frac{k_{mixture}}{k_{liquid}} = \frac{1-\varepsilon}{1-0.5\ln(1-\varepsilon)}, \qquad [4]$$

or the models derived by Yianatos, Laplante, Finch (1985) from geometrical analysis.

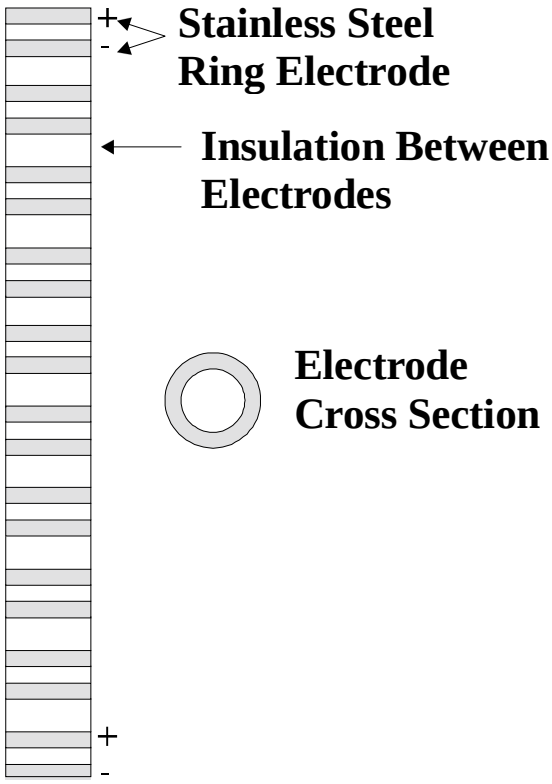

Figure 3.1: Ring Conductivity Probe Used to Study the Stabilized Froth

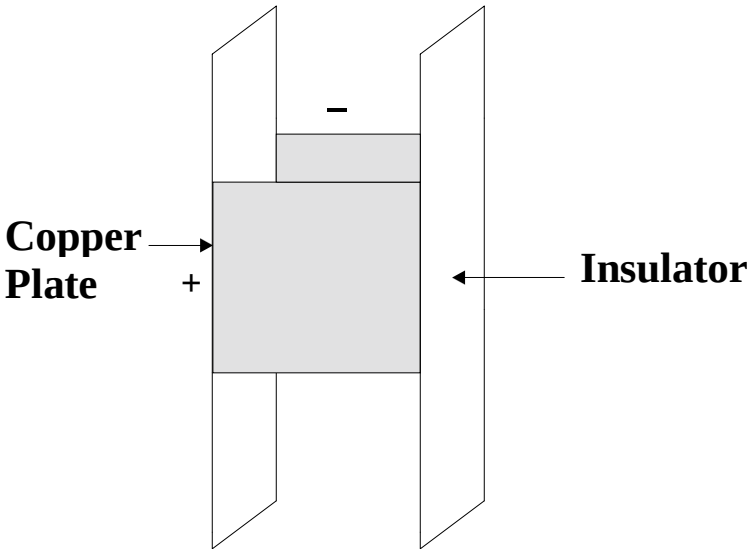

Figure 3.2: Conductivity Cell Used in the Study of the Draining Froth

The Maxwell model is applicable to spherical or closely spherical particles (or in this case, bubbles). Another model was developed by Fricke's (1924), which takes into account the particle shape. Banisi, Finch and Laplante (1994) compared some of the models using flake-shaped mica and graphite particles and measuring solid holdup with other techniques as well such as pressure difference and direct measurement by isolation. They concluded that the Maxwell model did not provide good predictions under those circumstances. On the other hand, Summers, Xu and Finch (1993) investigated the effect of using Maxwell's equation along with ring electrodes, since the Maxwell model requires a nearly uniform electric field. From that study, it appeared that the model was adequate for the estimation of air holdup with ring electrodes.

- *Interface / Stabilized Froth*

Several tests were carried out under different conditions in order to study changes in the stabilized froth profile and the behavior on both sides of the pulp-froth interface. The operating conditions for each of these tests are detailed in Table 3.1. The pulp air fraction values were obtained from averaged pressure-transducer measurements. The conductances measured by each electrode during the tests were normalized by dividing by the conductance measured with the corresponding electrode when the column was full of water only.

Table 3.1: Experimental Conditions During Air-Holdup Profile Measurements in Stabilized Froth

Test No.	Pulp Air Fraction	Air Rate	Frother	Wash Water	Froth Depth
1	15%	2000ml/m	0.020ml/m	400ml/min	30.5 cm
2	20%	1600ml/m	0.025ml/m	400ml/min	35.6 cm
3	11%	1600ml/m	0.017ml/m	400ml/min	35.6 cm
4	11%	1600ml/m	0.015ml/m	450ml/min	35.6 cm
5	28%	2000ml/m	0.025ml/m	400ml/min	35.6 cm

The conductance ratio profile derived from the first test is shown in Figure 3.3. The data indicate that the transition from a low air holdup, below the interface, to a high air holdup above is very sharp. Most of the increase takes place in a very small region around the interface. In contrast, the increase in air fraction above the interface appears to be rather small (an indication of froth stability), except for the measurement provided by the highest electrode. This last electrode happened to be located very close to the center of the wash water sprinkler, in a region where the water may be poorly distributed.

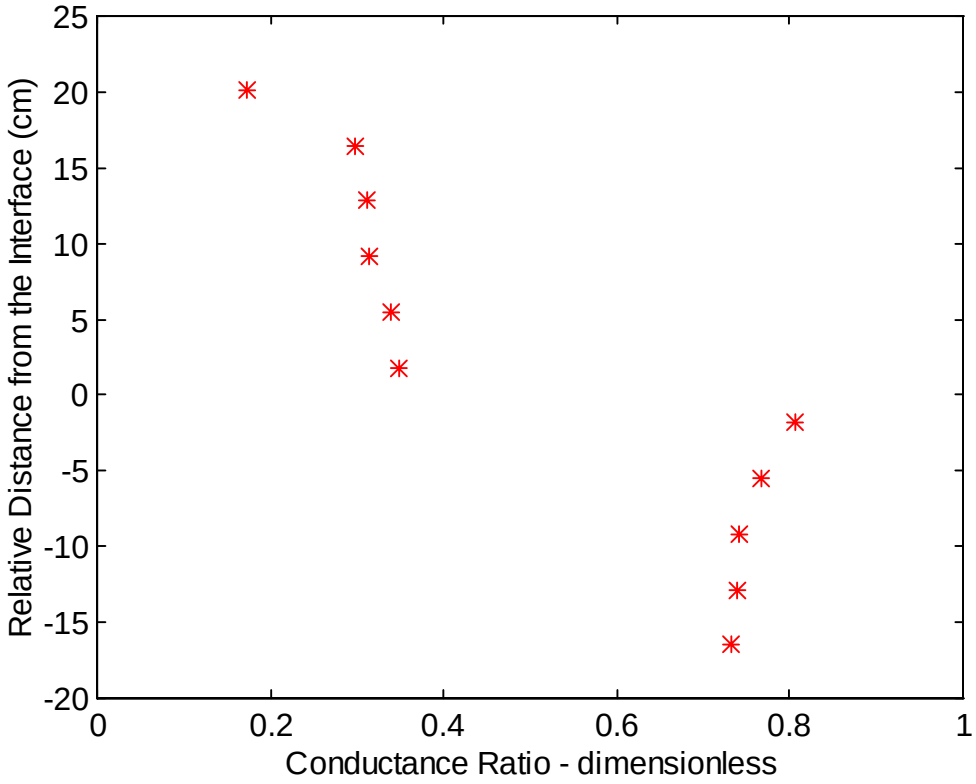

Figure 3.3: Conductance Ratio Profile obtained from Test No.1 (Two-Phase System)

In Figure 3.4, the ratios corresponding to Test No.2 are provided. It is readily observed that the average conductance in the collection zone is lower than in the previous test, indicating that the air fraction in the pulp is higher. In spite of the decrease in air rate (see Table 3.1), the increase in air fraction was a result of the higher frother rate used and the rise in liquid velocity required to maintain a deeper froth. The increase in frother rate caused a reduction in bubble size Meanwhile, the conductance ratio profile in the stabilized froth shifted to the right indicating a higher liquid content. The profile is very steep suggesting a very stable bubble size along the stabilized froth, which can be linked to the higher downward liquid flow.

For the third test, the frother rate was decreased while keeping air rate constant, and, as a result, the bubble size in the pulp increased. The experimental profile shows that the resulting reduction in pulp air fraction, as indicated by the increase in the conductance ratios, is associated with a much lower liquid content (average conductance ratio along the stabilized froth. This translates into a wider gap between the values on both sides of the interface in Figure 3.5. The further decrease in frother addition in Test No. 4, which should have resulted in an even drier froth, was seemingly compensated by an increase in

bias water (higher wash water rate). Therefore, the conductance ratio profile for the fourth test did not vary much from the one obtained in the previous run, as shown in Figure 3.6.

The shape of the profile in Figure 3.7, corresponding to Test No. 5, seems to indicate that the system was close to the flooding point. That point theoretically corresponds to the condition when the air fractions on both sides of the interface become equal and the pulp-froth interface disappears. The large pulp air fraction was the aftermath of an increase in both air rate and frother addition (listed in Table 3.1), which prompted a significant rise in the bubble surface area rate crossing the interface. The data points are also very dispersed, which could suggest that the system was departing from the bubbly flow regime.

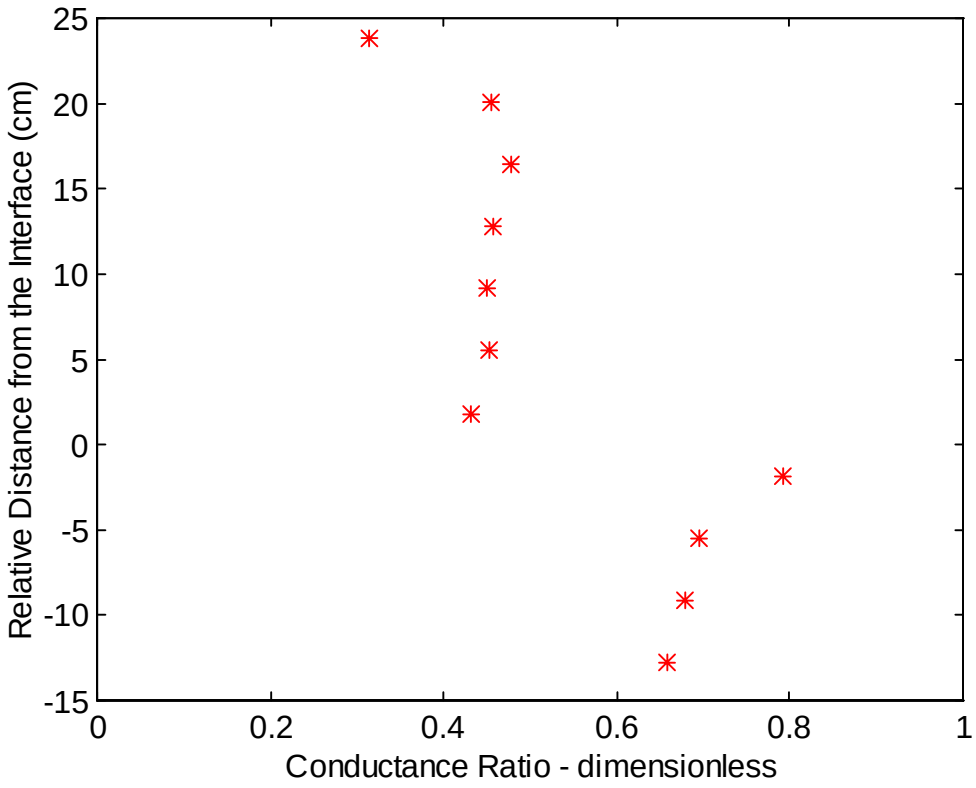

Figure 3.4: Conductance Ratio Profile obtained from Test No.2 (Two-Phase System)

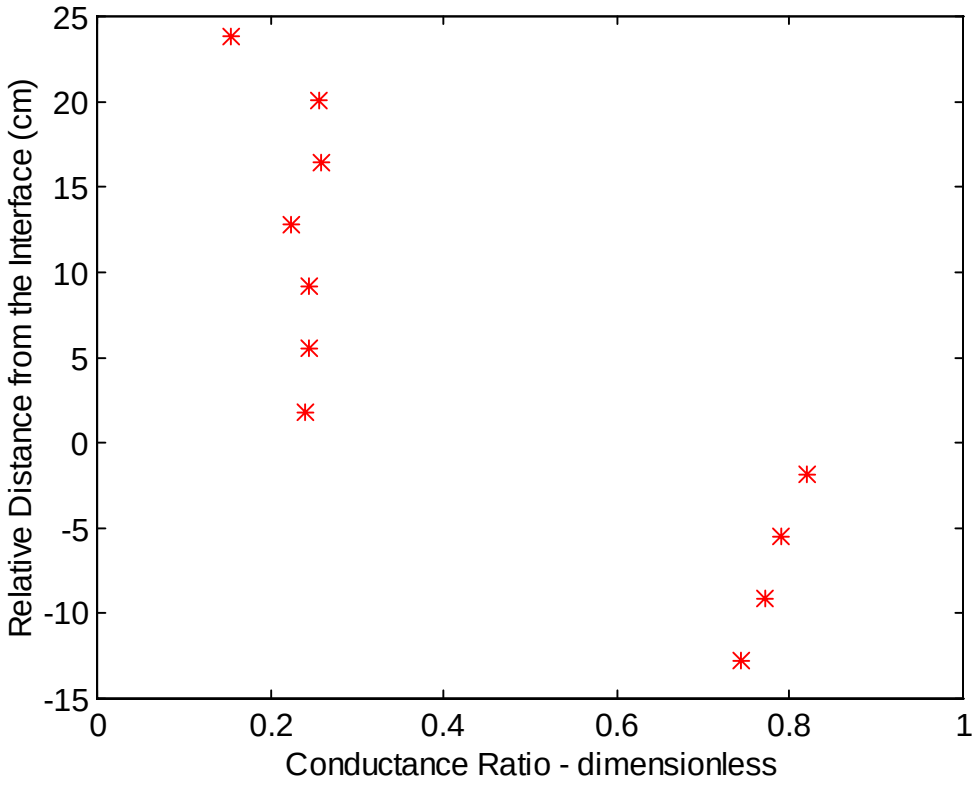

Figure 3.5: Conductance Ratio Profile obtained from Test No.3 (Two-Phase System)

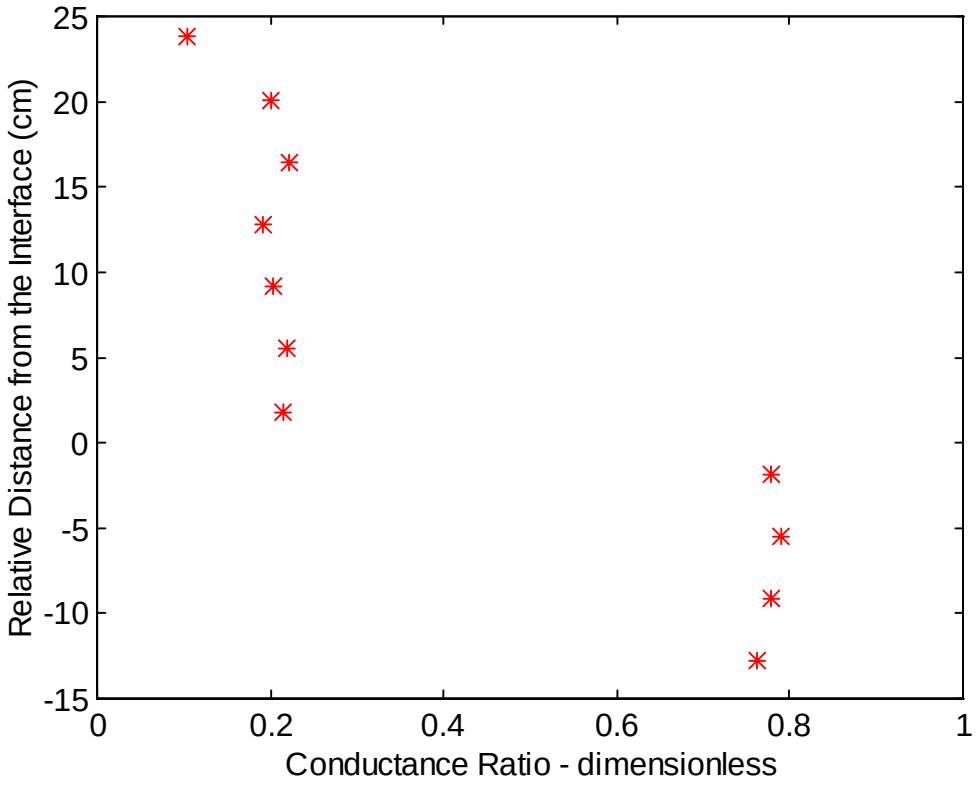

Figure 3.6: Conductance Ratio Profile obtained from Test No. 4 (Two-Phase System)

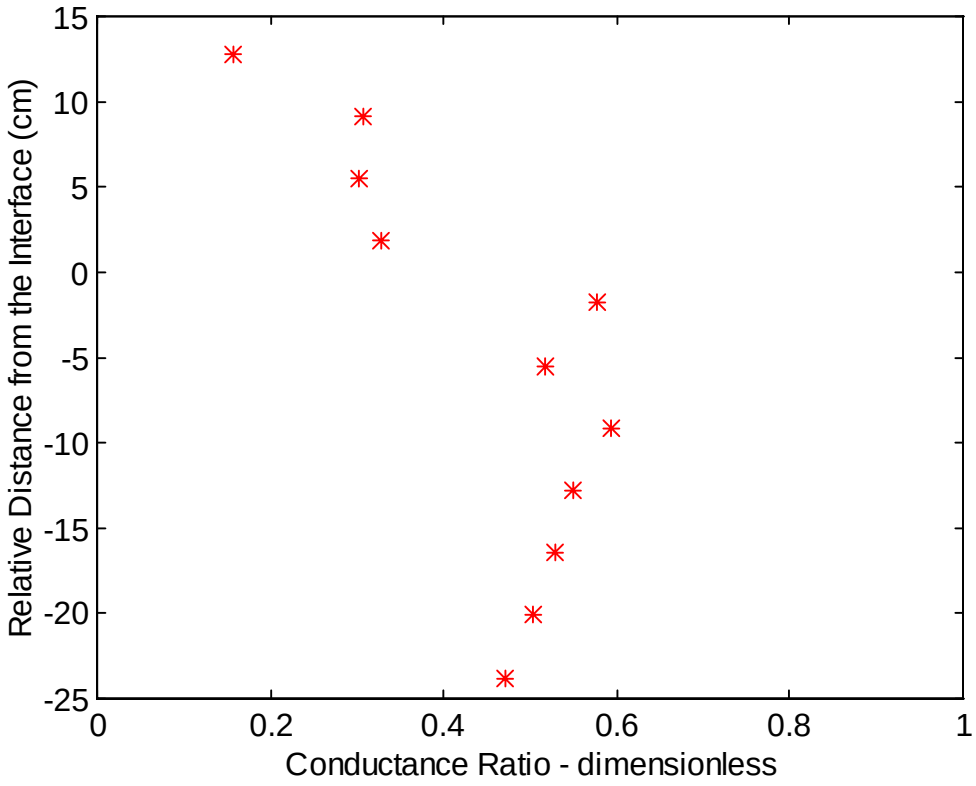

Figure 3.7: Conductance Ratio Profile obtained from Test No. 5 (Two-Phase System)

The experimental air fraction values in Table 3.1 were fitted to the average conductance ratio in the pulp using a more general form of Maxwell's equation:

$$\varepsilon = \left(\frac{1 - \frac{K_{air-water}}{K_{water}}}{1 + a \frac{K_{air-water}}{K_{water}}} \right) \qquad [5]$$

The parameter *a* was calculated through a nonlinear curve-fitting procedure using the five data sets from the tests. This procedure is based on a simplex algorithm for minimizing an error function. The value obtained was 1.074. The first column of Table 3.2 contains the average air fractions below the interface calculated using the modified Maxwell's equation, while the second column consists of the measurements performed with two pressure transducers.

Table 3.2: Comparison between Experimental and Calculated Pulp Air Fractions

	Calculated Air Fraction	Measured Air Fraction
Test 1	**14%**	**15%**
Test 2	**17%**	**20%**
Test 3	**12%**	**11%**
Test 4	**12%**	**11%**
Test 5	**29%**	**28.0%**

In order to estimate air fraction from the measurements above the interface, the Weissberg model was solved using a numerical technique to obtain ε from the equation given below:

$$\frac{k_{mixture}}{k_{liquid}} - 0.5 \frac{k_{mixture}}{k_{liquid}} \ln(1-\varepsilon) - 1 + \varepsilon = 0 \qquad [6]$$

This model was utilized for the froth regions because it was originally developed based on the assumption of overlapping spherical particles, which resembles better the conditions of bubble packing in a froth.

The calculated air fraction profile for the conditions in Test No.1 is shown in Figure 3.8. Overall, it can be seen that the air fraction profile looks like a mirror image of the conductance ratio profile. The air fractions above the interface are shown to range from 0.52 to 0.7. The calculated air fractions corresponding to Test No.2 are plotted in

Figure 3.9. In this case, the values derived from the calculations of air fraction in the stabilized froth are seemingly low (in the neighborhood of 0.45) in comparison to the normal range for a column froth, between 0.55 and 0.75.

In Test No. 3, a drier froth was observed, as illustrated by Figure 3.10, because the amount of entrained water was reduced by the increase in the size of the bubbles in the pulp. The calculated air fractions corresponding to Test No. 4, shown in Figure 3.11, do not differ significantly from those of the third test. The air fraction values in Figure 3.10 and Figure 3.11 are similar to the ones found in the literature for typical operating conditions in a flotation column (between 0.6 and 0.7). As it was noted before with respect to the conductance profiles, the calculated air fraction does not vary a lot along the stabilized froth. The measurements suggest that there is a significant increase in air fraction very close to the wash-water addition point. However, errors may have been introduced by the position of the highest electrode with respect to the wash water distributor. In the profile shown in Figure 3.12, where the transition from pulp to froth is not as readily distinguished, the difference between average air contents on both sides of the interface is around 20 %.

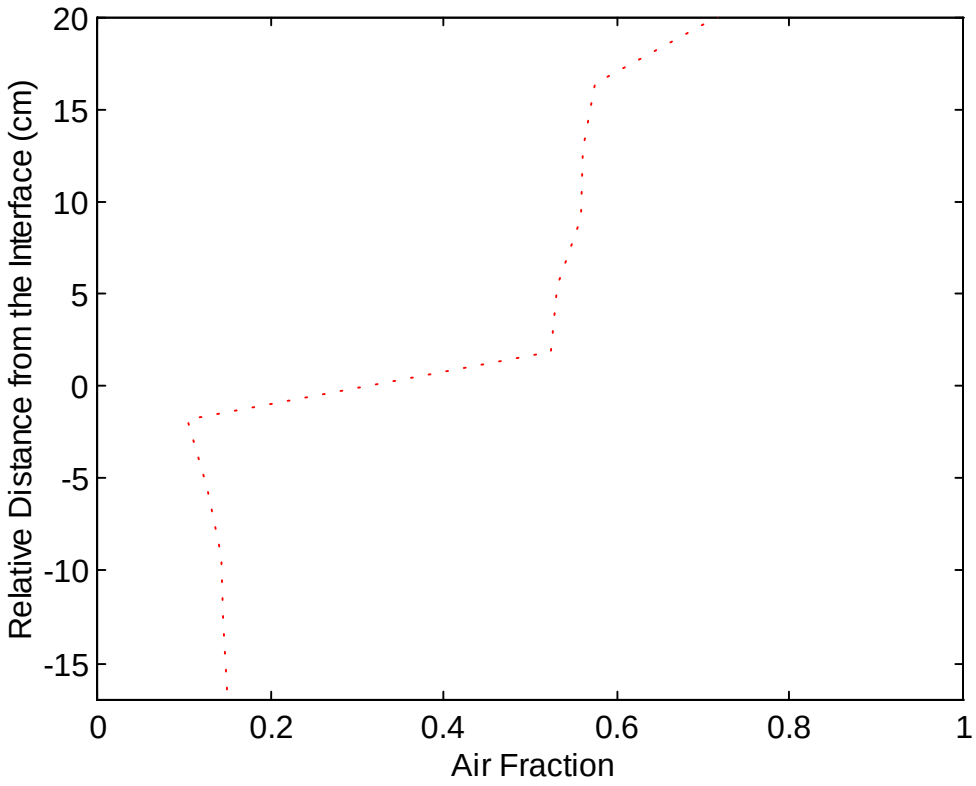

Figure 3.8: Calculated Air Fraction Profile Obtained From Conductivity Test No.1 (Two-Phase System)

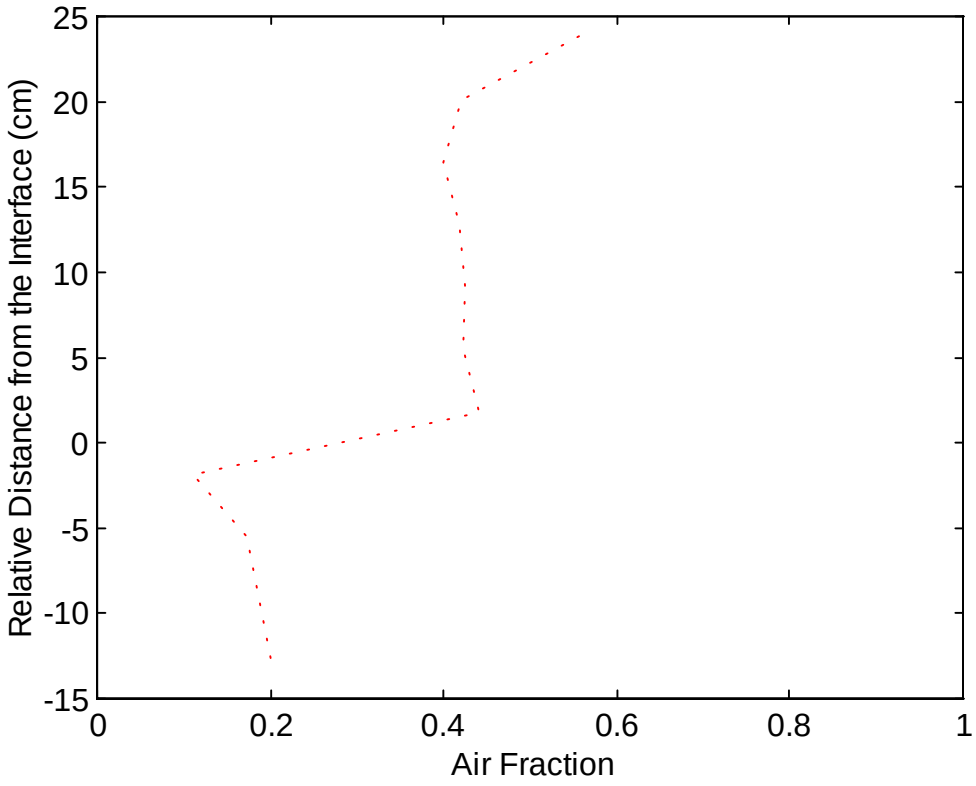

Figure 3.9: Calculated Air Fraction Profile Obtained From Conductivity Test No.2 (Two-Phase System)

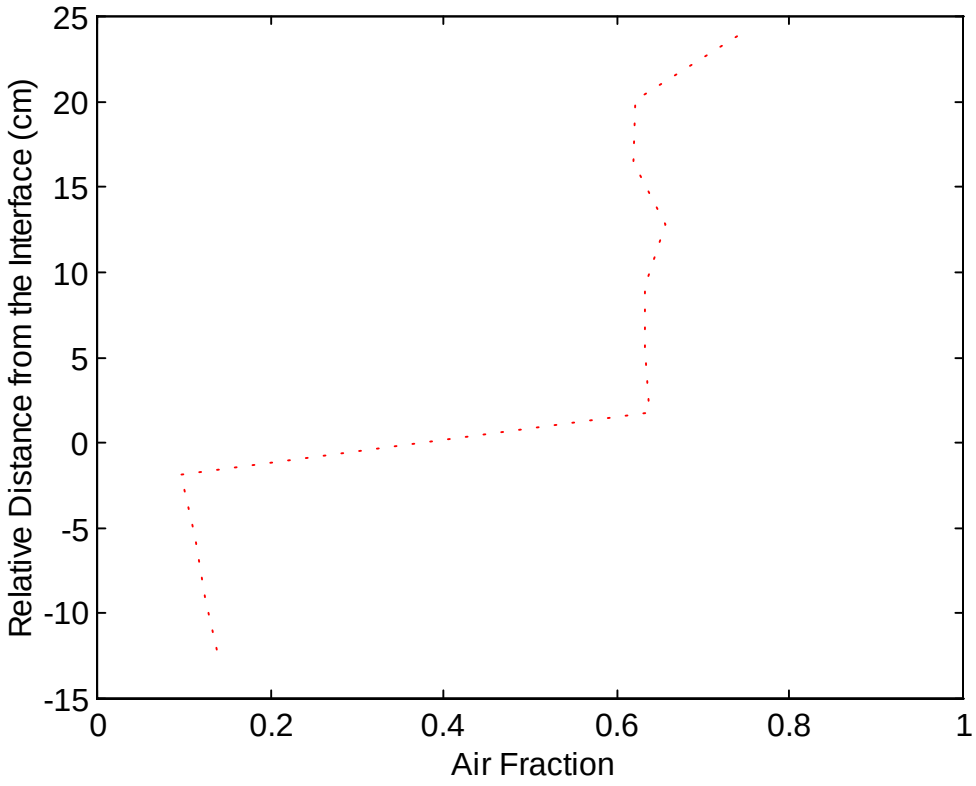

Figure 3.10: Calculated Air Fraction Profile Obtained From Conductivity Test No.3 (Two-Phase System)

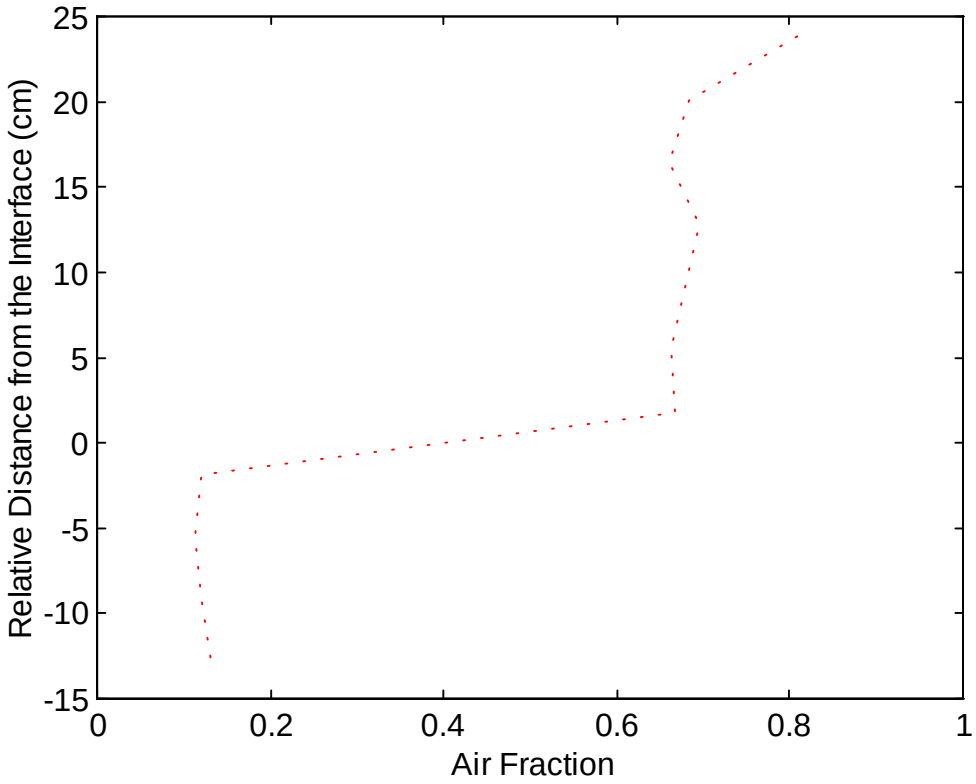

Figure 3.11: Calculated Air Fraction Profile Obtained From Conductivity Test No.4 (Two-Phase System)

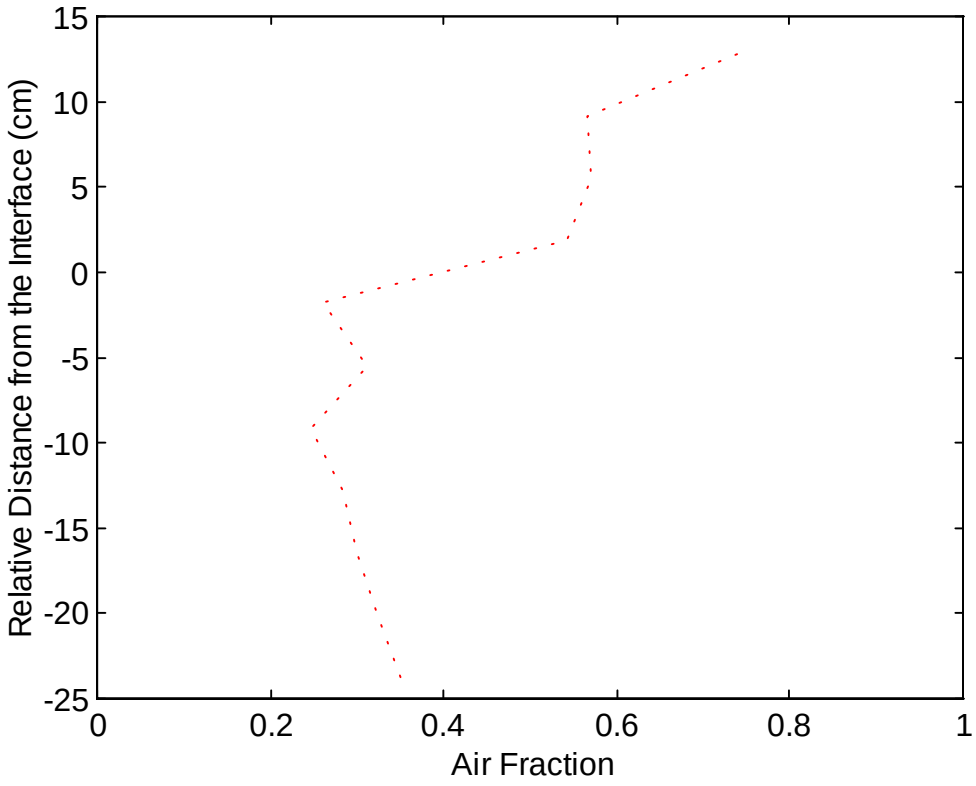

Figure 3.12: Calculated Air Fraction Profile Obtained From Conductivity Test No.5 (Two-Phase System)

- *Draining Froth*

In the case of the draining froth, it was necessary to use the smaller parallel-plate-type electrode due to limitations in froth depth. During the tests, the air rate and the position of the wash-water distributor were varied as indicated in Table 3.3 in order to observe how the air fraction profile in the draining froth is affected by these variables. Figure 3.13a shows the conductance ratio profile obtained for three different gas velocities and a froth depth of 4 centimeters, while Figure 3.13b provides the corresponding air fractions calculated using Weissberg's model. The experiment results indicate that the froth becomes wetter at higher aeration rates. Such conclusion is reasonable since the reduction in bias water caused by the increase in air rate translates into a higher liquid velocity in the concentrate. Froth drainage is consequently reduced, resulting in a wetter froth. Only two electrodes were used because of the limitation introduced by the physical size of the electrodes given the small depth of the zone.

Table 3.3: Experimental Conditions During Air-Holdup Profile Measurements in Draining Froth

Test No.	Froth Depth	Air Rate	Frother	Wash Water
1	4 cms	a) 1.2 cm/sec b) 1.5 cm/sec c) 1.7 cm/sec	0.025ml/m	400ml/min
2	6 cms	a) 1.2 cm/sec b) 1.5 cm/sec c) 1.7 cm/sec	0.025ml/m	400ml/min
3	8 cms	a) 1.2 cm/sec b) 1.5 cm/sec c) 1.7 cm/sec	0.025ml/m	400ml/min
4	8 cms	a) 1.2 cm/sec b) 1.5 cm/sec	0.050ml/m	400ml/min

In the next test, the froth depth was adjusted to 6 centimeters and the profile was measured using three electrodes for the three gas velocities recorded previously. The shape of the profile can be appreciated better in Figure 3.14a because one more cell was employed. Figure 3.14b suggest that in a two-phase draining froth the air fraction changes more rapidly at the base of the froth. The plots show again that higher gas velocities result in wetter froths (lower air fraction).

When the froth depth was increased to 8 centimeters and new measurements were obtained by using four electrodes, a more detailed profile was revealed, as shown in Figures 3.15a and 3.15b. It was noticed that the difference between the air fractions at the base and the top of the froth increased significantly as the froth became deeper. This can be observed by comparing the profiles for the 6-cm froth and the 8-cm froth. An

explanation for such behavior is that the deeper froth provides more opportunity for film drainage, resulting in a drier froth at the top with large deformed bubbles. The profiles in Figures 3.16a and 3.16b also correspond to an 8-cm-deep froth, but they were obtained at a frother concentration twice the one used in the previous tests (see Table 3.3). The general shape of the profile does not appear to change. Because of the high froth liquid content established by the increase in frother addition, the increase in air rate appears to have a lesser impact on froth air fraction than in the preceding test.

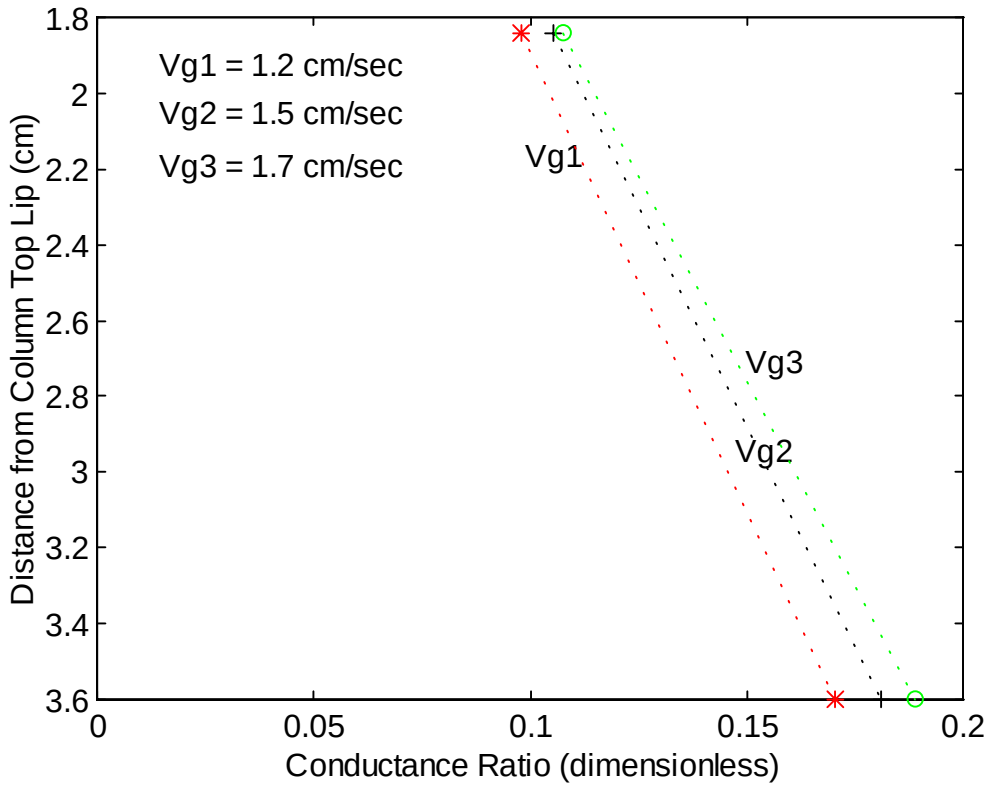

Figure 3.13a: Conductance Ratio Profiles in Two-Phase Draining Froth (Depth = 4 cm)

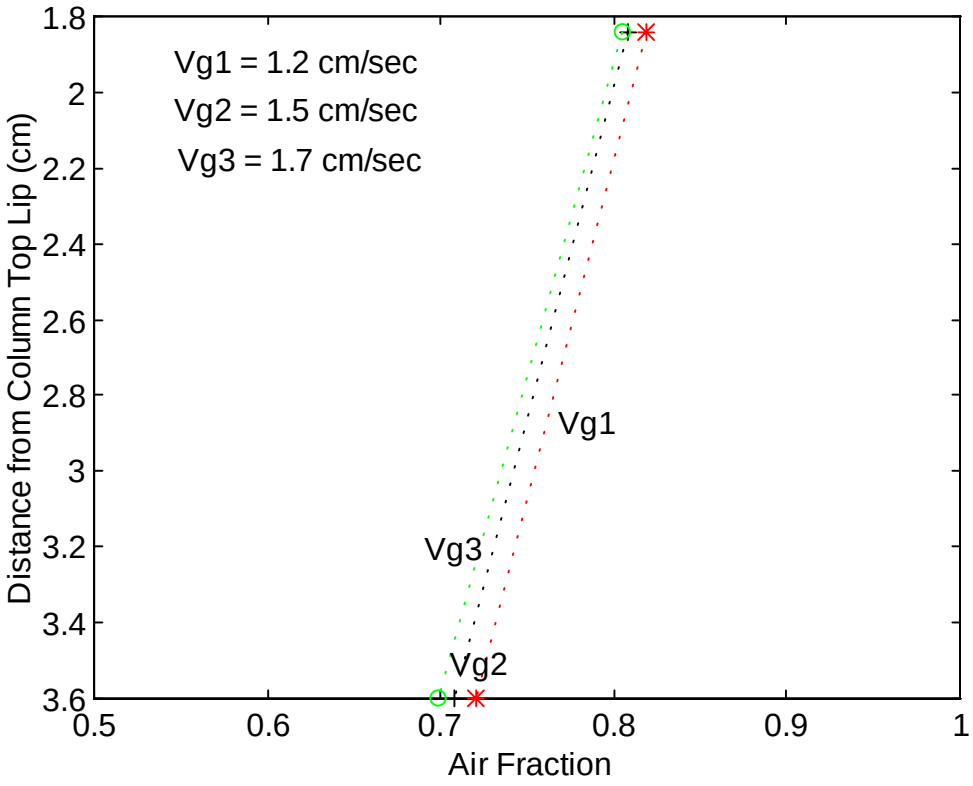

Figure 3.13b: Air Fraction Profiles in Two-Phase Draining Froth (Depth = 4 cm)

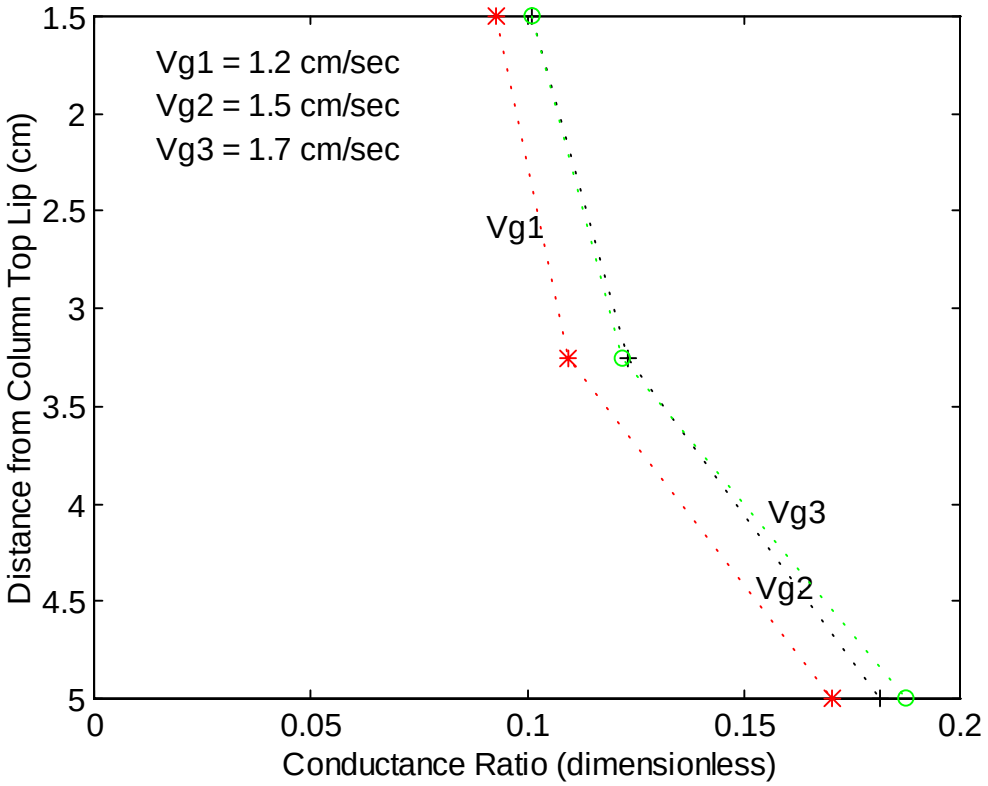

Figure 3.14a: Conductance Ratio Profiles in Two-Phase Draining Froth (Depth = 6 cm)

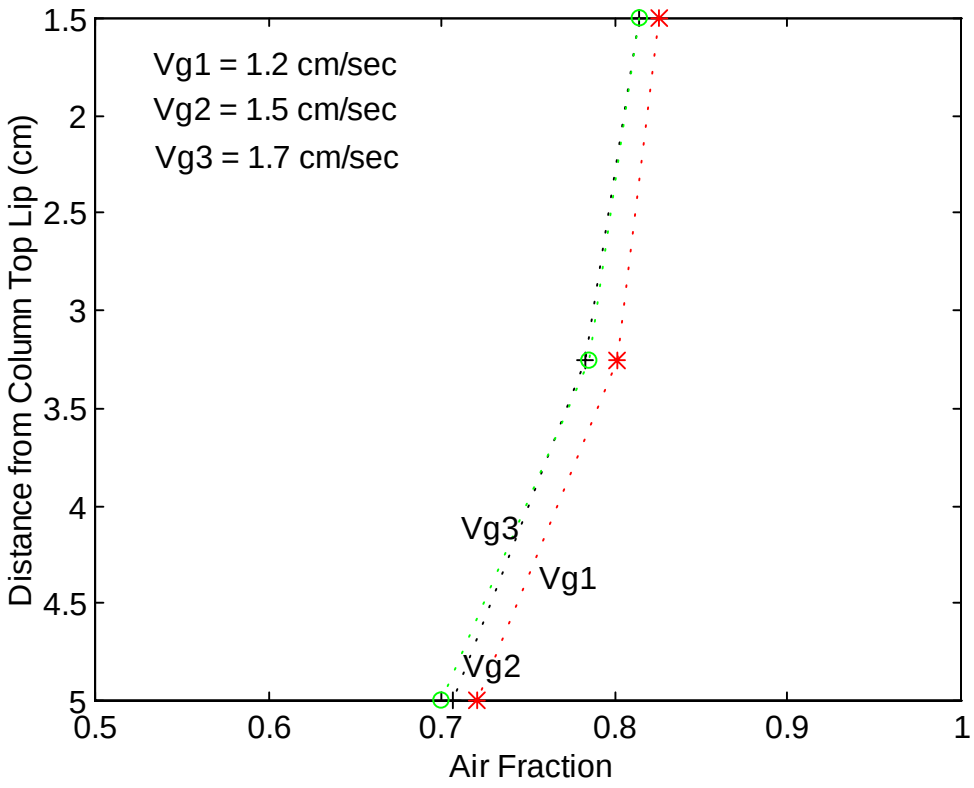

Figure 3.14b: Air Fraction Profiles in Two-Phase Draining Froth (Depth = 6 cm)

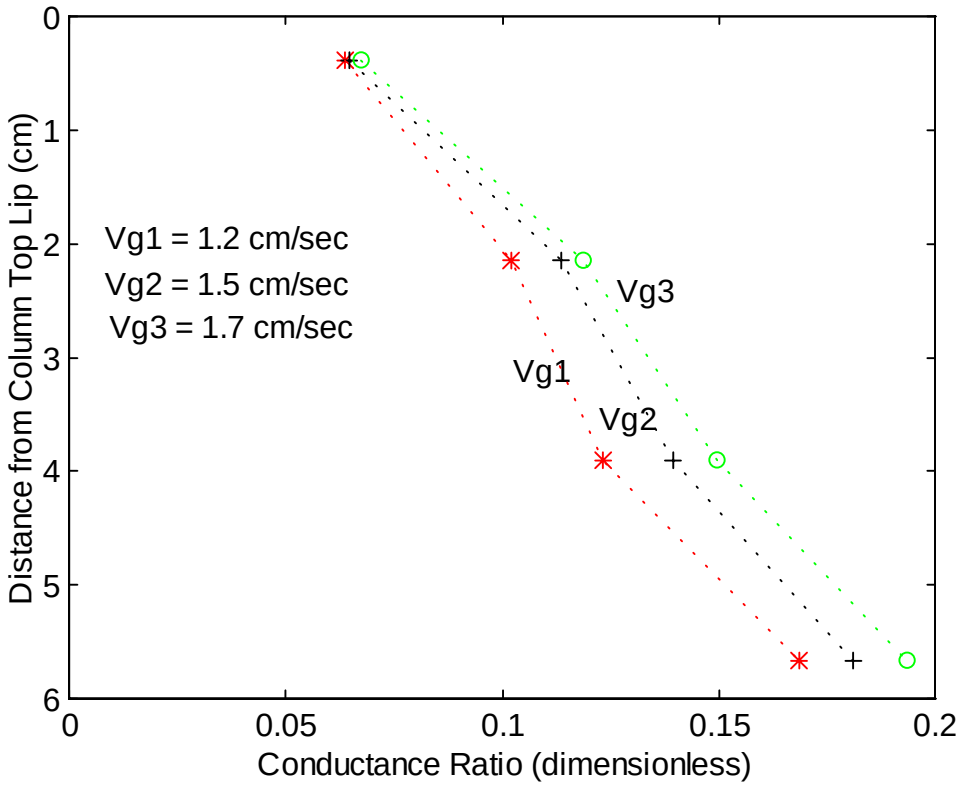

Figure 3.15a: Conductance Ratio Profiles in Two-Phase Draining Froth (Depth = 8 cm)

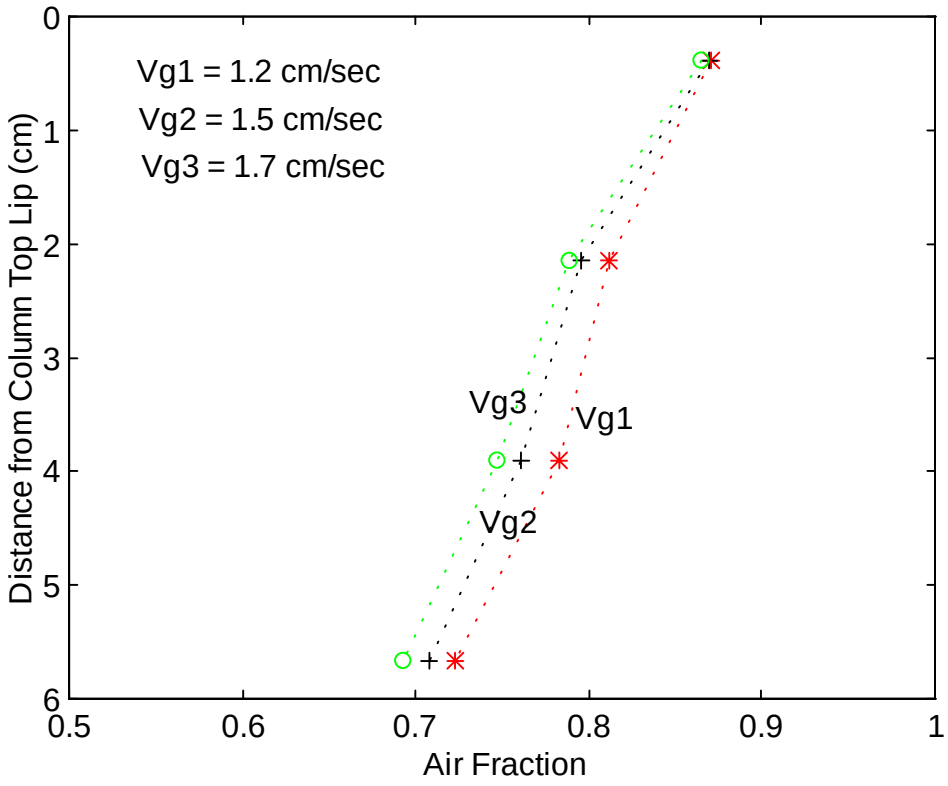

Figure 3.15b: Air Fraction Profiles in Two-Phase Draining Froth (Depth = 8 cm)

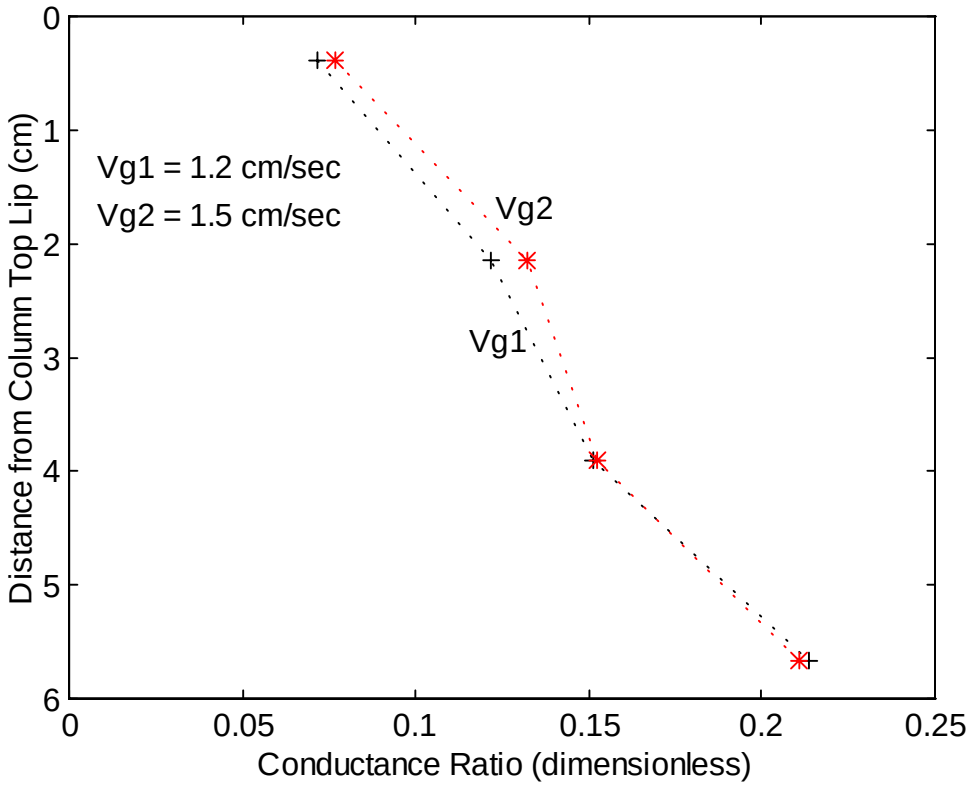

Figure 3.16a: Conductance Ratio Profiles in Two-Phase Draining Froth (Depth = 8 cm, Higher Frother Rate)

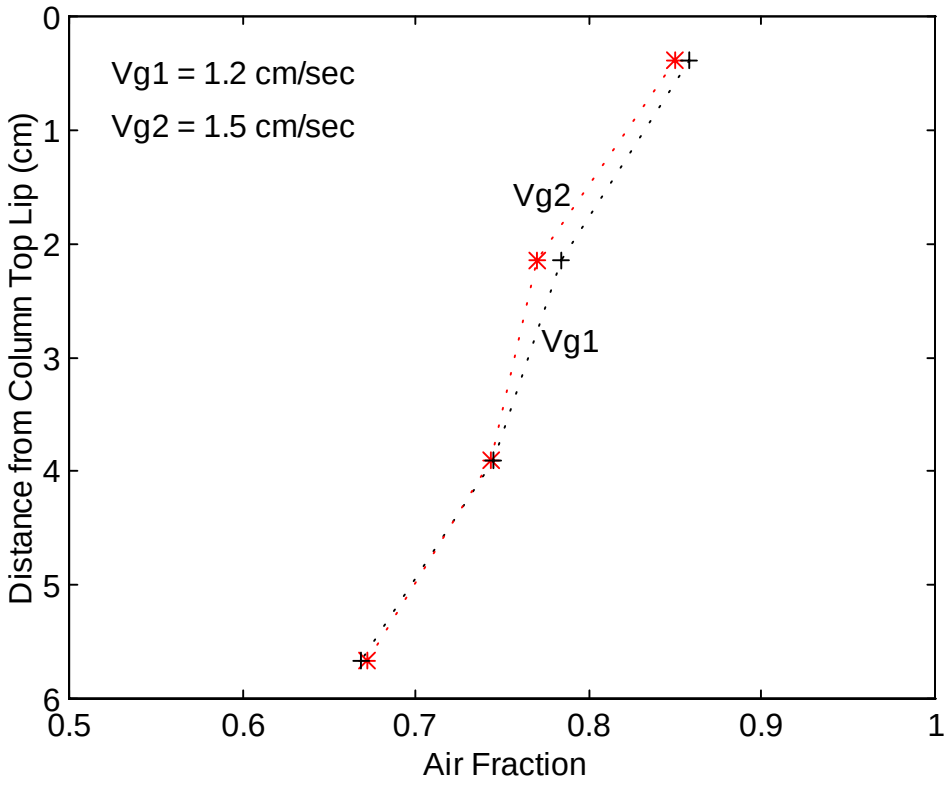

Figure 3.16b: Air Fraction Profiles in Two-Phase Draining Froth (Depth = 8 cm , Higher Frother Rate)

3.4 Three-Phase System

For the case of a three-phase froth, the conductivity of the solids-water mixture was the reference value, or denominator, in the calculation of the conductivity ratio. In order to determine the solids-water conductivity, small quantities of slurry were drawn out at several positions along the froth. The slurry conductance was then measured employing the same probe so that a constant electrode geometry was maintained.

In the draining froth, it was observed that the conductance of the slurry decreased along the froth, approaching the value measured in a concentrate sample. The reason appears to be mainly the decrease in water content at the top of the froth due to drainage. In the stabilized froth, the observed decrease in the solids-water conductance with height was small. Another factor that could contribute to the differences between the conductance measurements is the relative amount and composition of the solids in the slurry.

As with the air-water system, the ratio between the conductivity of an air-slurry solution and the conductivity of the slurry is a function of the air holdup and the tortuosity. The tortuosity is again defined as the relative increase in the length of the path between the electrodes due to the presence of air. The general functional form that relates air fraction to conductivity measurements is:

$$\varepsilon = 1 - \xi \frac{k_{3-\text{phase mixture}}}{k_{\text{slurry}}}, \qquad [7]$$

where ξ is the tortuosity term. Maxwell's equation (Equation [3]) and Weissberg's model (Equation [4]) are also applicable to three-phase processes.

- *Interface-Stabilized Froth*

The objective of determining the conductivity profile along a solids-laden stabilized froth was to investigate the effect of the presence of solids on the shape of the profile, in comparison to an air-water-frother froth. The probe was positioned inside a two-inch-diameter laboratory column and it extended below the pulp-froth interface. Conductance measurements for the slurry were obtained by extracting samples of material along the column froth while in operation. After the bubbles in the samples collapsed, the conductance of the slurry was measured using the probe. Two types of samples were used, both from the Middle Fork coal preparation plant, which is a property of Pittston Coal Co. One type is the feed to the flotation columns that are currently used at Middle Fork to treat material from a refuse pond. The ash content in this sample was 46%. The other type of sample used in the tests was obtained from the concentrate of the columns at

the same location. This coal sample had around 7% ash. Figure 3.17 provides a general schematic of the experimental setup.

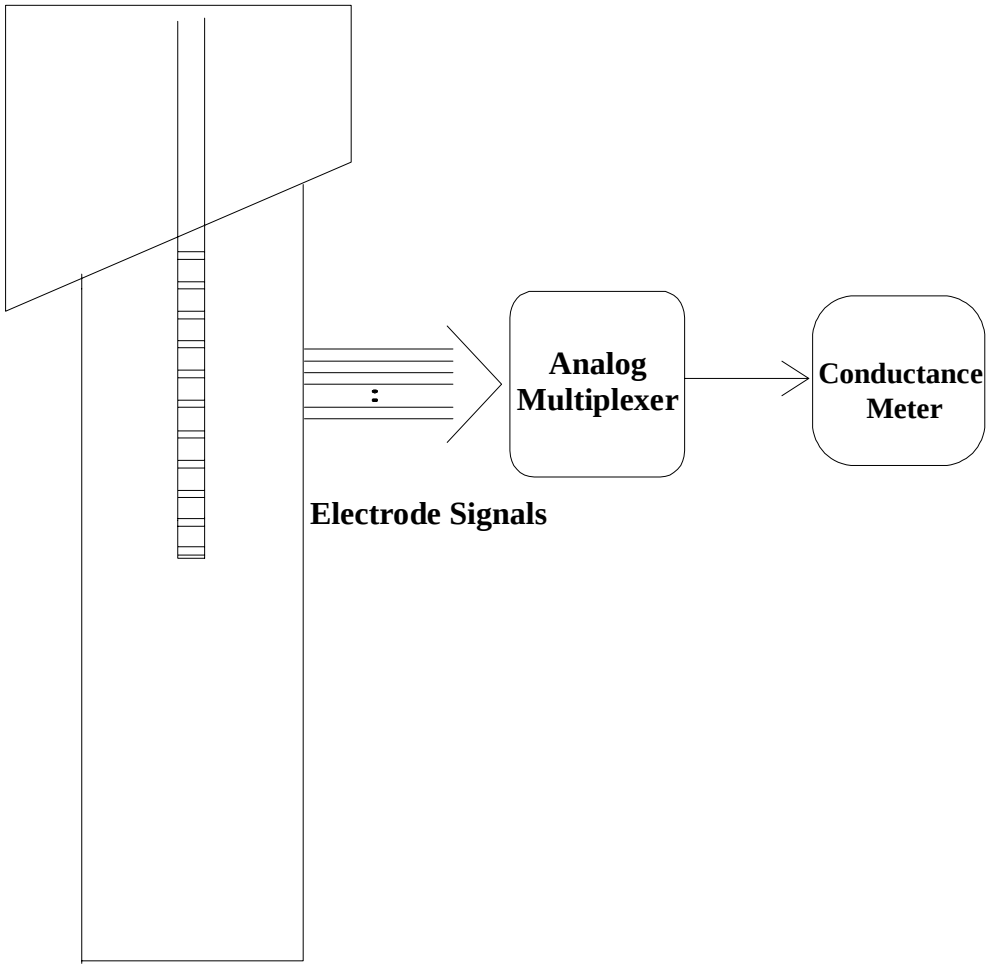

Figure 3.17: Experimental Setup for Determining Air Fraction Profile in Column Stabilized Froth Using a Conductivity Probe

Three tests were performed with the operating conditions provided in Table 3.4. During the first two tests, the column was fed with the 46%-ash slurry. The conductance values, measured with and without air, are given in Table 3.5, along with the ratios and the estimated air fractions. The Maxwell model was found to predict too high air fraction values, particularly for the column stabilized froth region, which is characterized by high

liquid content. The estimates provided by the application of Weissberg's equation were lower, although this equation sometimes yielded values above 0.80. Weissberg's equation has been found to be more appropriate for the estimation of air fraction in froths (high air fractions) due to its treatment of the bubbles as overlapping spheres (Yianatos, Laplante and Finch, 1985).

Table 3.4: Experimental Conditions During Air-Holdup Profile Measurements in Three-Phase Stabilized Froth

Test No.	Air Rate	Frother	Wash Water	Feed Rate	Froth Depth
1	4.5 ml/m	0.030 ml/m	400ml/min	2.2	31 cm
2	5.0 ml/m	0.030 ml/m	400ml/min	2.3	33 cm
3	4.5 ml/m	0.025 ml/m	400ml/min	1.5	33 cm

Table 3.5: Measurements Obtained in the Stabilized Froth during Test No.1 for Each of the Eleven Electrodes (with Solids)

Electrode No. (from bottom)	Conductance Three-Phase Froth	Slurry Conductance	Ash	Conductance Ratio	Estimated Air Fraction
1	300.0	421	-	0.713	0.205
2	277.7	-	-	0.660	0.247
3	307.3	421	-	0.730	0.192
4	285.0	-	-	0.699	0.216
5	280.8	408	45.8	0.688	0.225
6	292.8	-	-	0.718	0.201
7	20.25	181	-	0.112	0.798
8	15.25	-	-	0.090	0.830
9	11.90	171	-	0.070	0.861
10	9.21	-	-	0.066	0.867
11	5.34	139	6.7	0.038	0.915

In order to be able to compare the results from the various tests, the conductance measurements were translated into air fractions using Equation [6]. The conductance

ratios for the set of eleven electrodes are represented in Figure 3.18 while the resulting air fraction profile is shown in Figure 3.19. The plots illustrate the transition between a relatively constant conductance ratio (air fraction) in the pulp region to a much lower ratio (higher air fraction) in the stabilized froth. Above the small region where the transition takes place, the decrease in the measured conductance with column height occurs smoothly and is of relatively small magnitude.

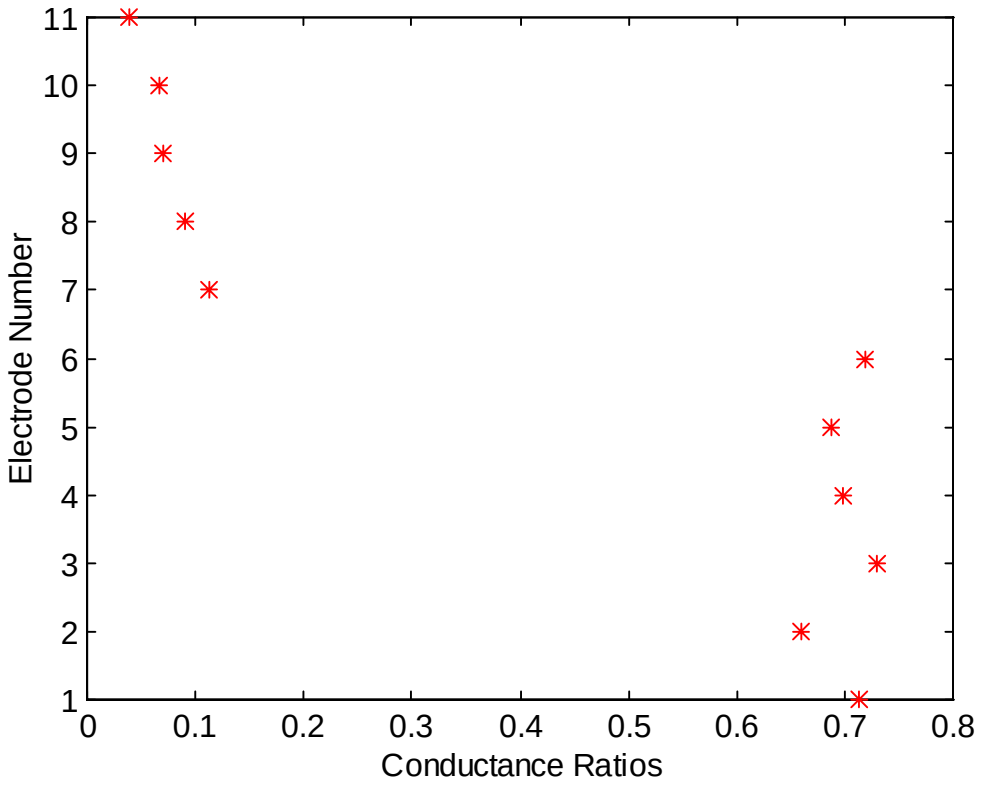

Figure 3.18: Conductance Ratios along the Stabilized Froth Corresponding to Test No.1 (with Solids)

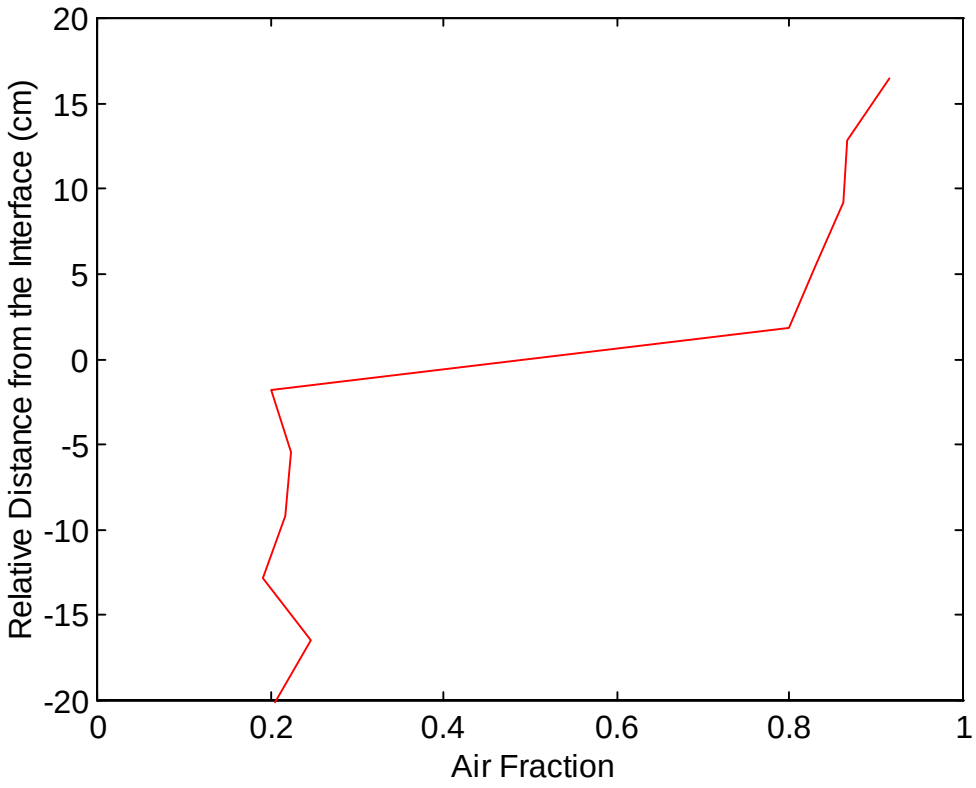

Figure 3.19: Estimated Air Fraction Profile in the Stabilized Froth for Test No.1 (with Solids)

After the pulp air fraction was increased, by raising the gas rate, the conductance values measured by the transducers located below the interface decreased, while the values measured above the interface increased slightly. Table 3.6 summarizes the obtained measurements with the corresponding air fractions calculated using Weissberg's model. The conductance ratios along the probe length and the estimated air fractions, for the new gas rate, are graphically represented with respect to the electrode positions in Figure 3.20 and Figure 3.21, respectively. In general, the sharp transition at the interface observed in the two-phase column does not appear to be altered by the transport of solids. The average conductance values (indicator of the air fraction) on both sides of the interface are a function of the operating conditions.

Table 3.6: Measurements Obtained in the Stabilized Froth during Test No.2 for Each of the Eleven Electrodes (with Solids)

Electrode No. (from bottom)	Conductance Three-Phase Froth	Slurry Conductance	Ash	Conductance Ratio	Estimated Air Fraction
1	226.0	322	-	0.702	0.214
2	210.5	-	-	0.695	0.219
3	211.7	-	-	0.699	0.216
4	219.7	303	-	0.725	0.196
5	221.7	299	54.1	0.741	0.184
6	29.22	-	-	0.155	0.741
7	15.85	189	-	0.084	0.839
8	12.30	-	-	0.077	0.850
9	11.54	160	12.1	0.072	0.858
10	7.85	-	-	0.055	0.885
11	5.97	144	9.5	0.041	0.91

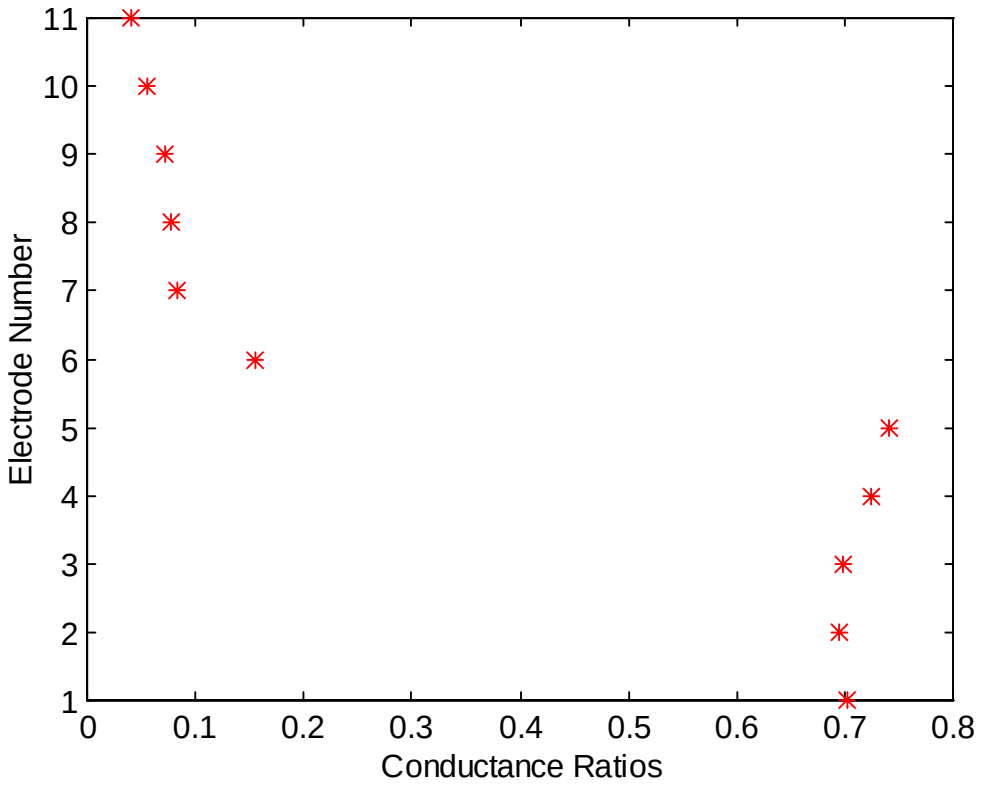

Figure 3.20: Conductance Ratios along the Stabilized Froth Corresponding to Test No.2 (with Solids)

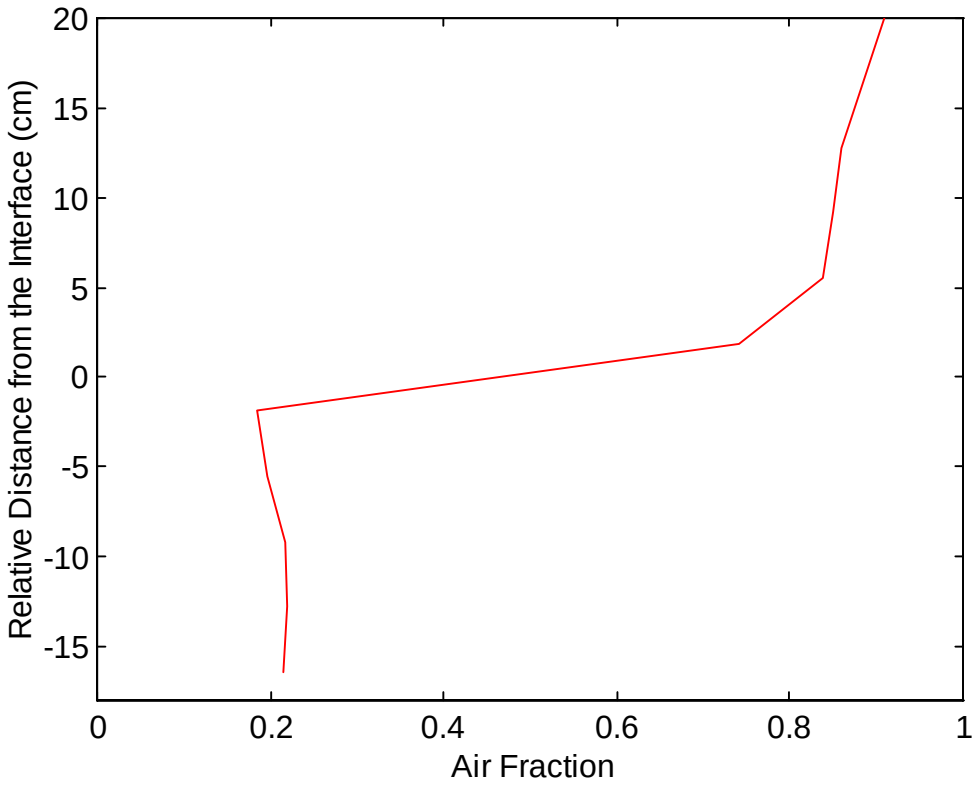

Figure 3.21: Estimated Air Fraction Profile in the Stabilized Froth for Test No.2 (with Solids)

In the next set of tests, the column was fed with the clean coal slurry (7% ash). With the lower feed rate (other conditions stayed about the same), the bubbles were not fully loaded, which was apparent in the high froth mobility throughout the test and the higher conductance values, as indicated in Table 3.7. The calculated froth air fractions are therefore lower than in the two preceding experiments, since the presence of solids on the bubbles affects the bubble size (by preventing coalescence) and their rise velocity. With regard to the slurry samples, there was not any significant change in slurry conductivity along the froth. The ash contents for the samples taken at different froth depths indicate that no upgrading took place. The conductance ratios and the air fraction profile are plotted in Figures 3.22 and 3.23, respectively.

Table 3.7: Measurements Obtained in the Stabilized Froth during Test No.3 for Each of the Eleven Electrodes (with Solids)

Electrode No. (from bottom)	Conductance Three-Phase Froth	Slurry Conductance	Ash	Conductance Ratio	Estimated Air Fraction
1	141.2	203	-	0.695	0.219
2	128.2	-	-	0.664	0.243
3	125.6	-	-	0.651	0.254
4	131.9	-	-	0.683	0.228
5	130.3	193	-	0.675	0.235
6	35.38	144	8.1	0.246	0.631
7	31.37	152	7.7	0.207	0.676
8	26.89	-		0.191	0.696
9	25.92	141	7.3	0.184	0.704
10	23.01	138	7.2	0.167	0.725
11	11.26	118		0.096	0.821

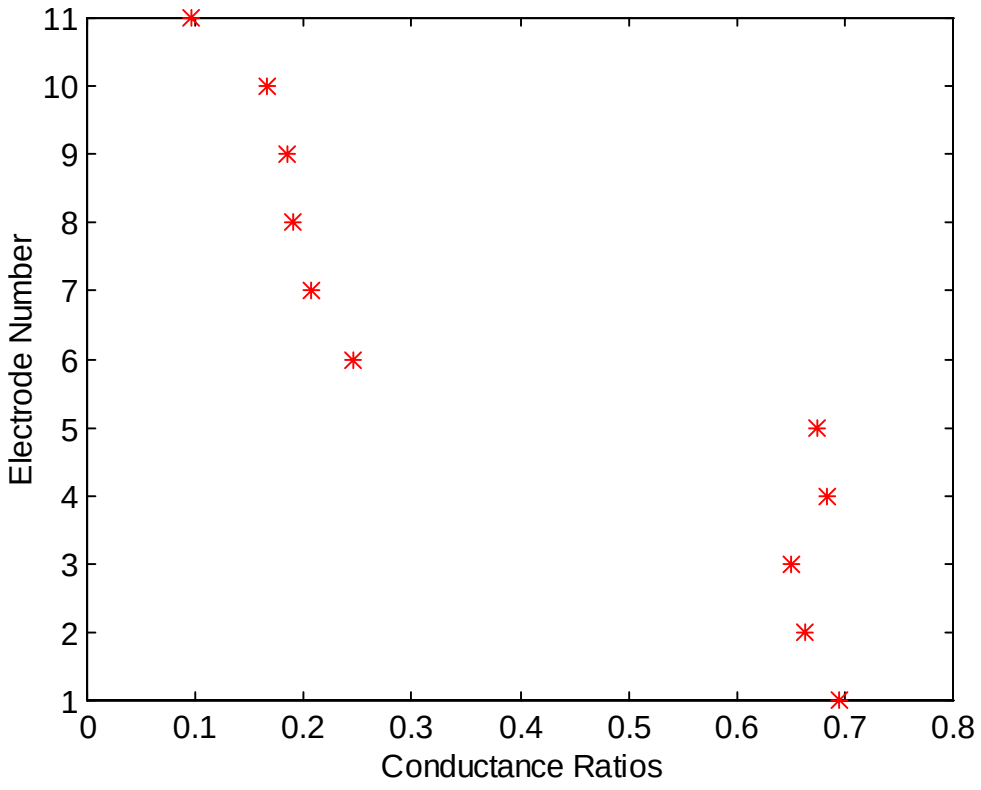

Figure 3.22: Conductance Ratios along the Stabilized Froth Corresponding to Test No.3 (with Solids)

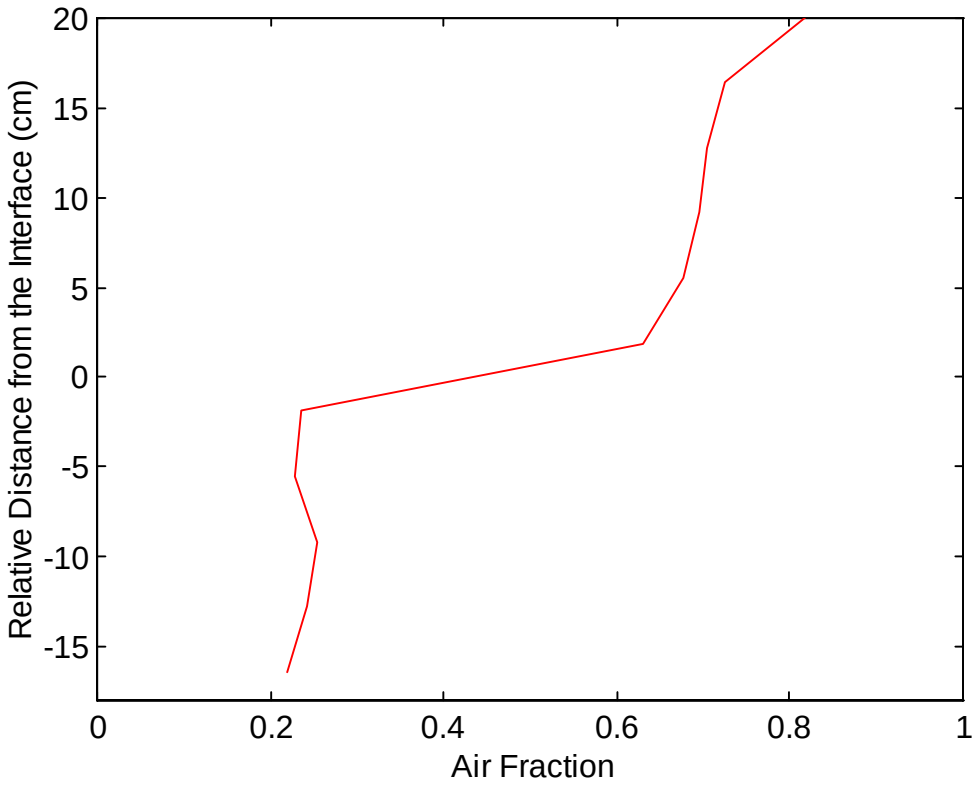

Figure 3.23: Estimated Air Fraction Profile in the Stabilized Froth for Test No.3 (with Solids)

In conclusion, it was observed that the particular conductance values may vary depending on the amount and type of solid material, but the shape of the profile in the stabilized froth is not noticeably affected by the solids.

- *Draining Froth*

The very low liquid content in the draining froth makes conductivity measurements difficult and the deposition of solids on the electrode surfaces can introduce significant errors. A large number of experimental tests were carried out at different operating conditions, such as feedrate, air rate and frother addition, to determine the changes in the air fraction profile as these parameters vary. The experimental setup is illustrated in Figure 3.24, and the various changes in operating parameters are explained in Table 3.8.

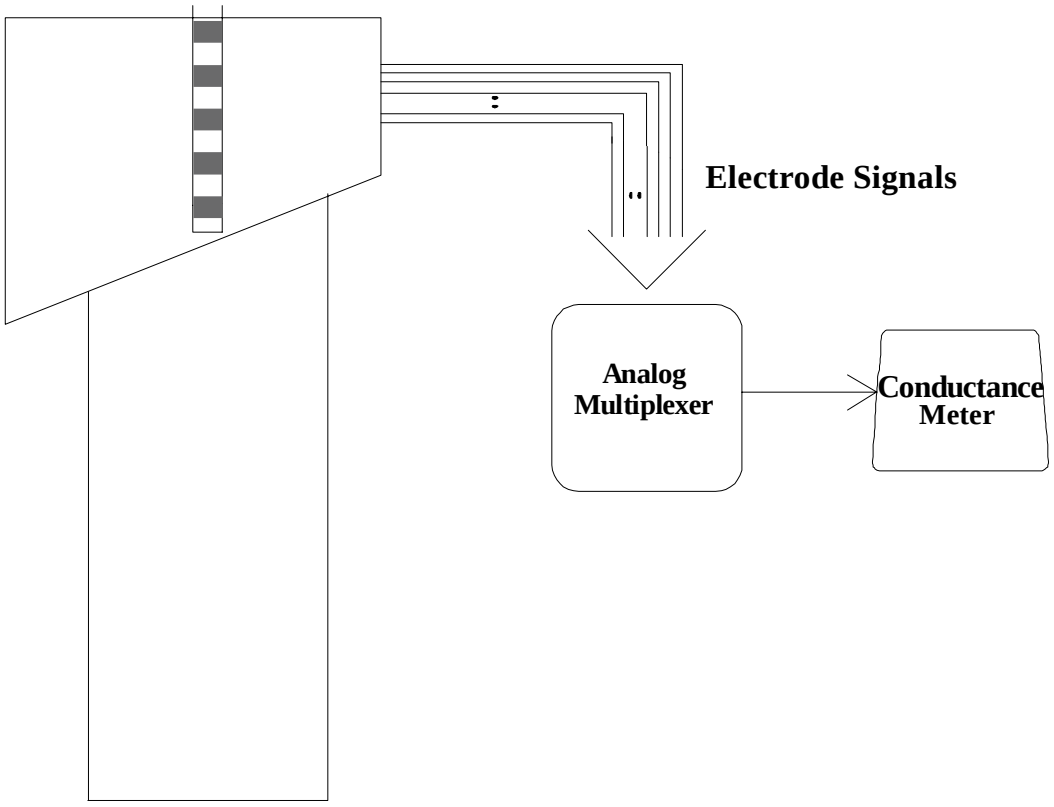

Figure 3.24: Experimental Setup for Determining Air Fraction Profile in Column Draining Froth Using a Conductivity Probe

Table 3.8: Experimental Conditions During Air-Holdup Profile Measurements in Three-Phase Draining Froth

Test No.	Feed Velocity	Air Velocity	Frother Rate	Wash Water Rate
1	0.08 cm/sec	1.5 cm/sec	a) 0.030ml/m b) 0.038ml/m b) 0.043ml/m	400ml/min
2	0.14 cm/sec	1.2 cm/sec	a) 0.033ml/m b) 0.038ml/m	400ml/min
3	0 cm/sec	1.5 cm/sec	a) 0.025ml/m b) 0.043ml/m	400ml/min
4	a) 0.04 cm/sec b) 0.06 cm/sec c) 0.075 cm/sec d) 0.082 m/sec	1.5 cm/sec	0.043 ml/m	400ml/min
5	a) 0.16 cm/sec b) 0 cm/sec	1.2 cm/sec	0.028 ml/min	400 ml/min
6	a) 0 cm/sec b) 0.08 cm/sec	1.5 cm/sec	0.048 ml/min	400 ml/min
7	a) 0 cm/sec b) 0.06 cm/sec c) 0.08 cm/sec	1.5 cm/sec	0.048 ml/m	400 ml/min
8	0.14 cm/sec	a) 1.2 cm/sec b) 1.5 cm/sec	0.033 ml/min	400 ml/min
9	0 cm/sec	a) 1.5 cm/sec b) 1.7 cm/sec	0.025 ml/m	400 ml/min

The experiments were repeated a number of times to verify consistency in the shape of the profiles observed. First, the frother addition rate was increased in steps and the electrode measurements were recorded each time. The set of air fraction profiles predicted using Weissberg's model for various frother rates are shown in Figure 3.25. The conductance values are larger, generally, for higher frother concentrations. This is explained by the increase in liquid content as the bubbles became smaller and carried more water to the froth. The bias rate was reduced, which implied a higher liquid rate flowing up the draining froth since the wash water rate was kept constant. A similar conclusion is derived from an analysis of Figure 3.26, which shows two profiles for constant operating conditions but different frother addition rates.

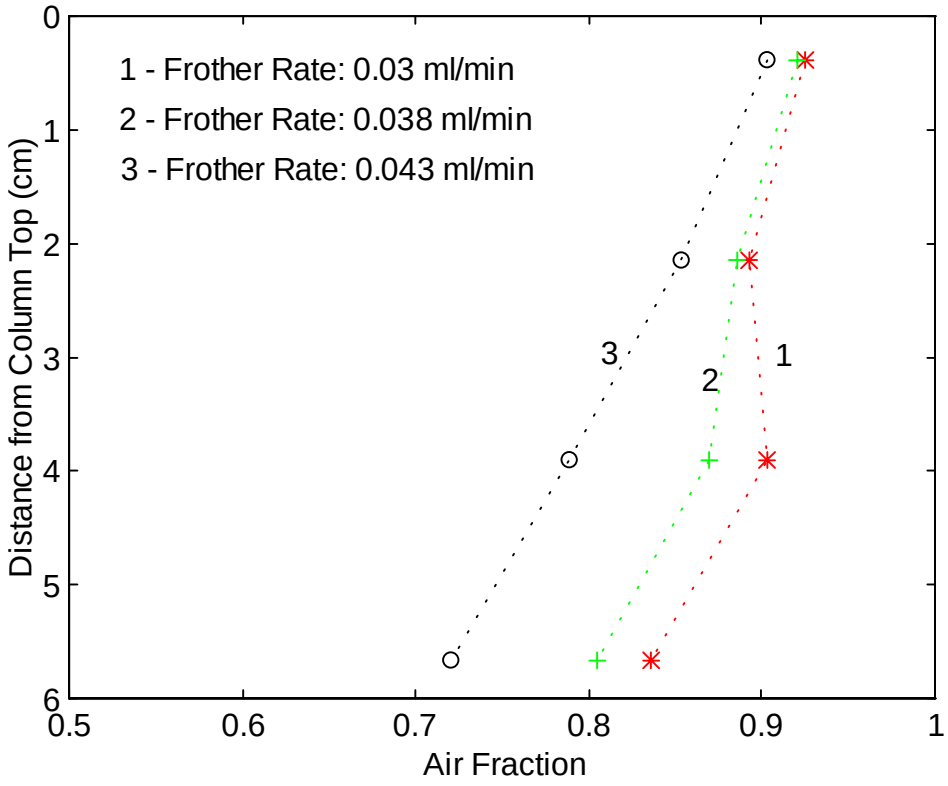

Figure 3.25: Air Fraction Profiles in the Three-Phase Draining Froth Determined with a Conductivity Technique for Various Frother Addition Rates

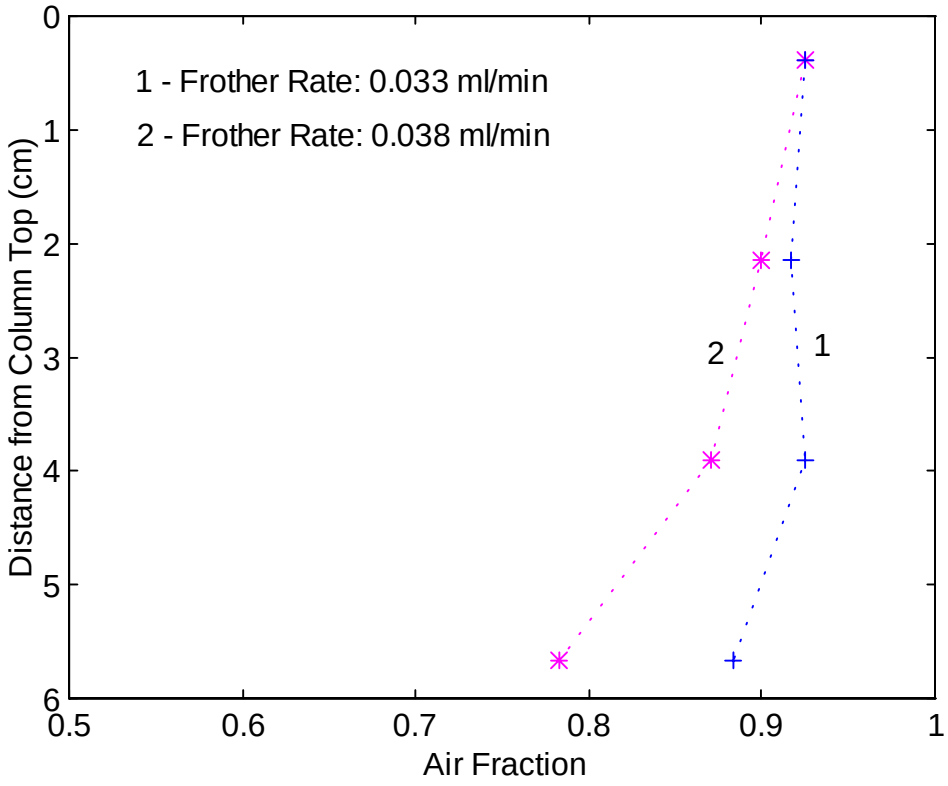

Figure 3.26: Air Fraction Profiles in a Three-Phase Draining Froth for Two Distinct Frother Addition Rates

If the profile shapes for a three-phase froth are compared with the ones obtained when there are no solids in the column (Figure 3.27), it is observed that when the froth is not loaded with particles, the profile tends to be S-shaped. Also, the net increase in air fraction along the froth is invariably larger in a lightly loaded or barren froth.

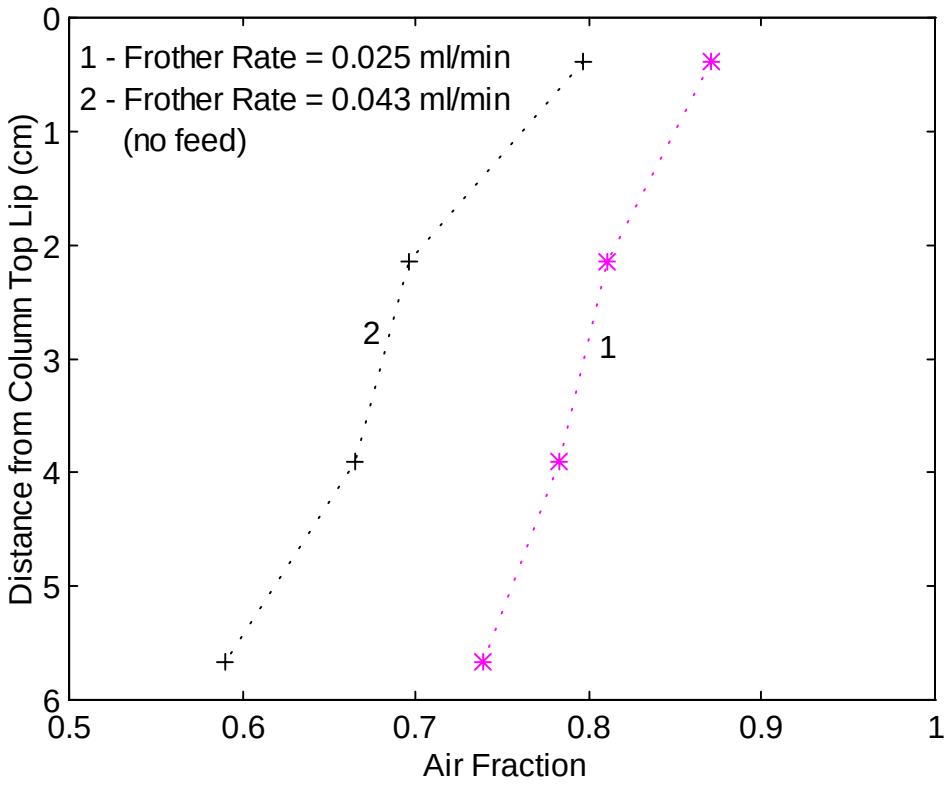

Figure 3.27: Air Fraction Profiles in a Two-Phase Draining Froth for Two Distinct Frother Addition Rates

In another set of experiments, the feed rate was changed in small steps. The profiles shown in Figure 3.28 indicate that at higher feed rates, as the froth becomes more loaded, the air fraction along the draining froth approaches a high but nearly constant value. It appears that the solids help establish a minimum film thickness that prevents drainage beyond a certain point. At a low superficial feed velocity of 0.04 cm/sec, the froth is very lightly loaded and the air fraction profile resembles the S-shape previously observed in the two-phase froths and plotted in Figures 3.29-3.31. These three plots show the results of additional tests performed to verify the effect of solids on the profile. The conclusions derived from the analysis of these profiles are:
a) as feed rate increases, the average air fraction along the draining froth increases; and
b) as solids loading increases, the air fraction profile becomes steeper because the presence of the particles reduces liquid drainage.

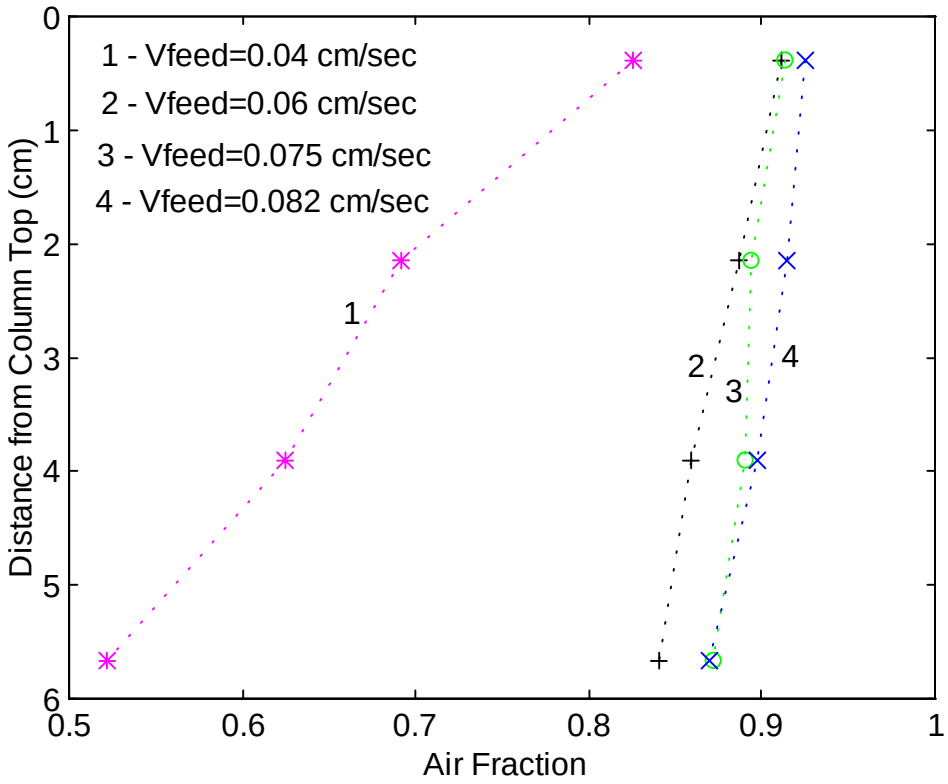

Figure 3.28: Air Fraction Profiles in the Three-Phase Draining Froth Determined with a Conductivity Technique for Various Feed Rates

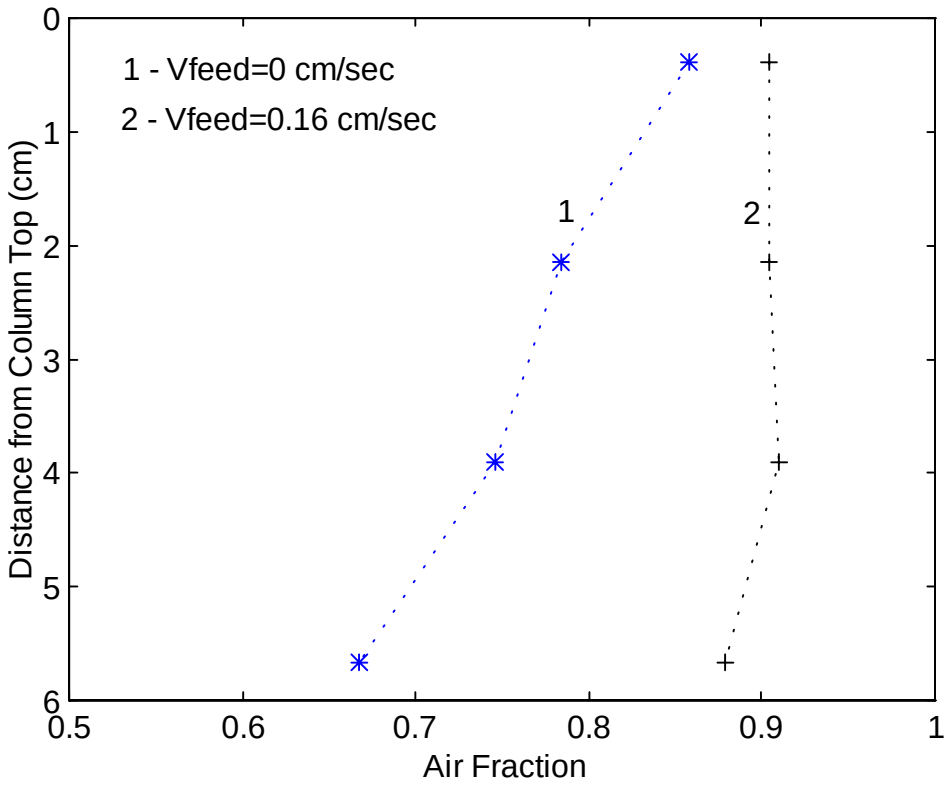

Figure 3.29: Air Fraction Profiles for a Two-Phase Draining Froth, and for a Three-Phase Froth with a Column Superficial Feed Velocity = 0.16 cm/sec.

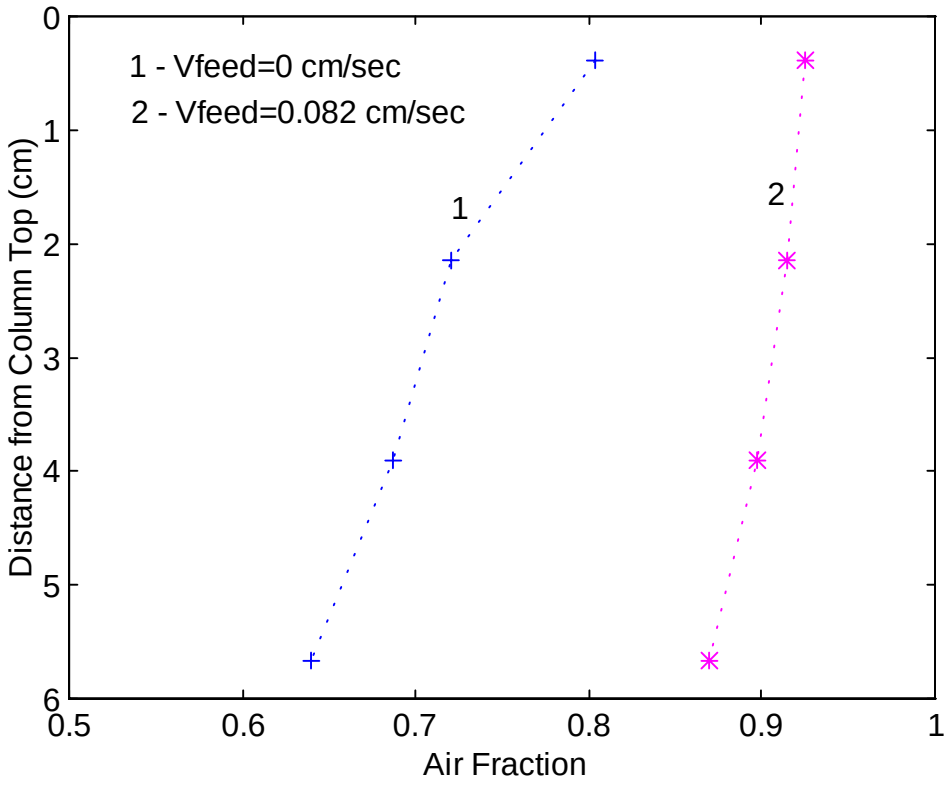

Figure 3.30: Air Fraction Profiles for a Two-Phase Draining Froth and for a Three-Phase Froth with a Column Superficial Feed Velocity = 0.08 cm/sec

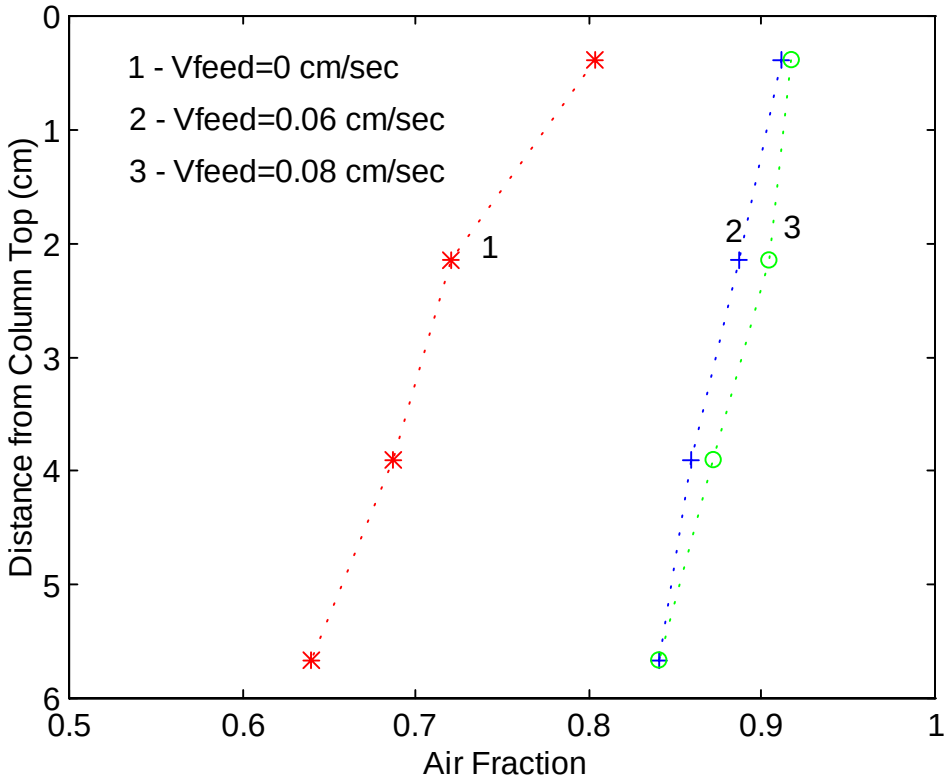

Figure 3.31: Air Fraction Profiles for a Two-Phase Draining Froth and for Two Other Three-Phase Froths with Different Column Feed Rates

It was also detected that, for increasing feed rates, the shift of the profile toward higher air fraction values became less noticeable. During this study, it was found that changes in air fraction in the draining froth were better appreciated using the conductivity method if the froth was not heavily loaded. Measurements in a froth with high solids content resulted in low conductance values independent of the other conditions. The reason appeared to be that the particles tended to accumulate on the electrode surfaces and could not be transported over the column.

Finally, the air rate was varied while keeping the other conditions constant. It was expected that an increase in air rate would also increase entrainment and, therefore, the liquid content in the froth. The effects observed were consistent with this prediction. The profiles corresponding to two different air rates, for a three-phase froth, are provided in Figure 3.32, while the profiles for a two-phase system at the same two air rates are illustrated in Figure 3.33. A significant difference in the shape of the profiles can be readily noticed when comparing both figures, which supports the forementioned conclusions about the solids effects.

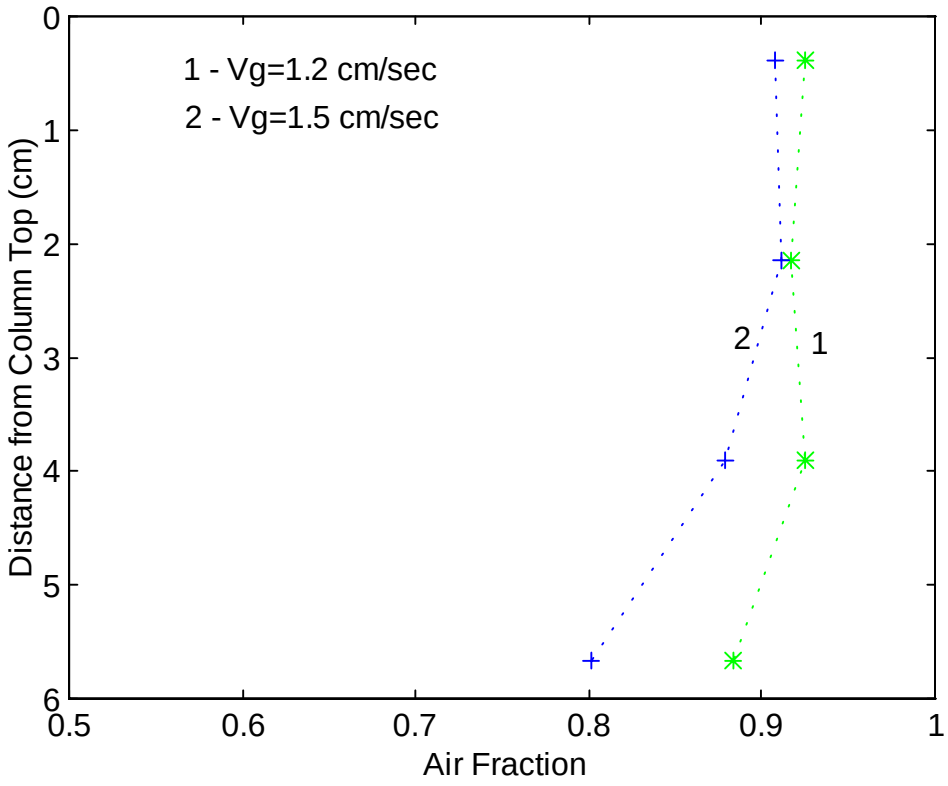

Figure 3.32: Air Fraction Profiles in a Three-Phase Draining Froth for Two Distinct Air Rates

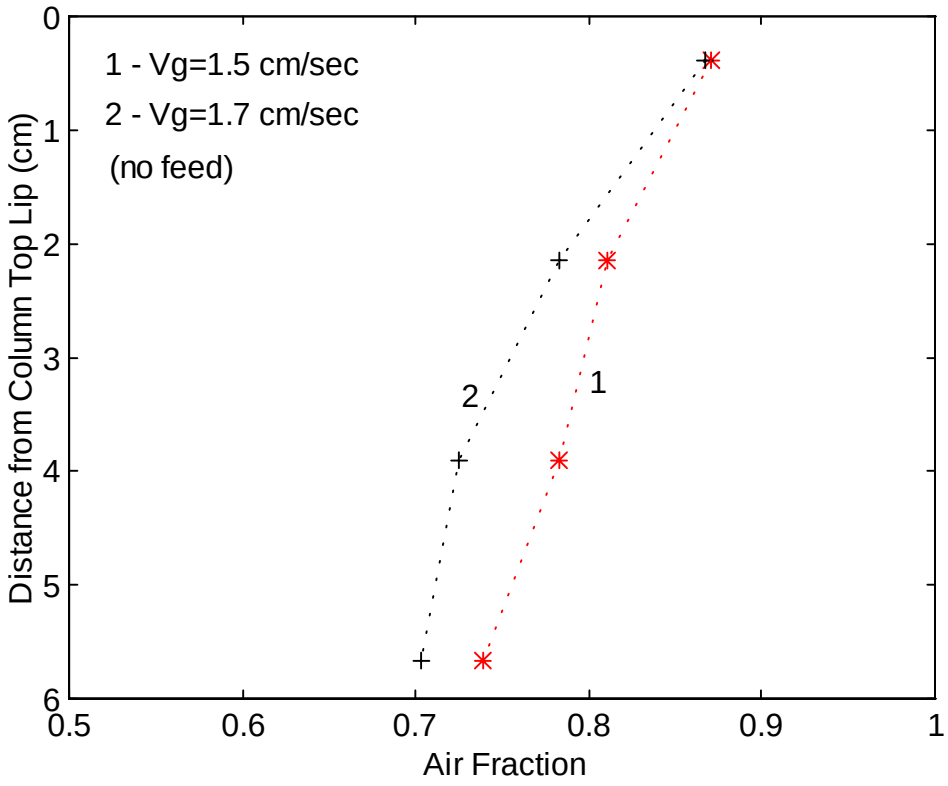

Figure 3.33: Air Fraction Profiles in a Two-Phase Draining Froth for Two Distinct Air Rates

3.5 Conclusions

- Conductivity techniques were applied in a study of the air fraction profiles along the froth phases of a flotation column. Two conductivity probe designs were employed mainly because of the differences in depth and liquid content between the stabilized froth and the draining froth. The effect of solids was investigated by comparing the profiles obtained in a two-phase system versus those from a column floating coal samples under similar conditions of gas, frother and wash water rates.

- It was observed that the transition to a high air fraction at the base of the froth occurs abruptly and that the increase in air holdup along the stabilized froth appears to be small. The profiles in the draining froth indicate that the deeper the froth, the larger the increase in air fraction throughout the region, which suggests a higher degree of coalescence due to drainage.

- The extent of the changes in air fraction due to coalescence in a three-phase stabilized froth, as well as the profile shape, does not differ from that associated with a two-phase froth. The main reason appears to be that the effect of the bias water in limiting coalescence overshadows the influence the presence of solids may have on the profile. The average air fraction value, not the shape of the profile, is a function of operating conditions.

- Under conditions when the draining froth is 'wetter', such as at high frother addition rates and low solids loading, the empirical air fraction profile displayed a notable increase from the bottom to the top of this column region. The profile resembles an S-shaped curve. For well-loaded froths, however, the net changes in air fraction along the draining froth are of small magnitude and the profile appears almost upright. It is suggested that the presence of solids reduces the rate of film drainage by setting a limit on the extent of film thinning.

- An important factor to consider is that conductivity measurements in a heavily loaded froth are complicated by the deposition of solids between the electrode faces.